A putative microcin amplifies Shiga toxin 2a production of *Escherichia coli* O157:H7

Running Title: Putative microcin amplifies Stx2a of O157:H7

Hillary M. Figler[a], Lingzi Xiaoli[b], Kakolie Banerjee, Maria Hoffmann[c], Kuan Yao[c], Edward G. Dudley[bd#]

[a] The Huck Institutes of the Life Sciences, The Pennsylvania State University, University Park, PA 16802

[b] Food Science Department, The Pennsylvania State University, University Park, PA 16802

[c] Center for Food Safety and Nutrition, U.S. Food and Drug Administration, College Park, MD

[d] Director of the *E. coli* Reference Center, The Pennsylvania State University, University Park, PA 16802

[#] Edward G. Dudley, egd100@psu.edu

Abstract word count: 315

Text word count: 5028

* Lingzi Xiaoli: Division of Bacterial Diseases, Centers for Disease Control and Prevention, Atlanta, Georgia 30333. Kakolie Banerjee: MilliporeSigma, Bedford, MA 01730

Abstract

Escherichia coli O157:H7 is a foodborne pathogen, implicated in various multi-state outbreaks. It encodes Shiga toxin on a prophage, and Shiga toxin production is linked to phage induction. An *E. coli* strain, designated 0.1229, was identified that amplified Stx2a production when co-cultured with *E. coli* O157:H7 strain PA2. Growth of PA2 in 0.1229 cell-free supernatants had a similar effect, even when supernatants were heated to 100°C for 10 min, but not after treatment with Proteinase K. The secreted molecule was shown to use TolC for export and the TonB system for import. The genes sufficient for production of this molecule were localized to a 5.2 kb region of a 12.8 kb plasmid. This region was annotated, identifying hypothetical proteins, a predicted ABC transporter, and a cupin superfamily protein. These genes were identified and shown to be functional in two other *E. coli* strains, and bioinformatic analyses identified related gene clusters in similar and distinct bacterial species. These data collectively suggest *E. coli* 0.1229 and other *E. coli* produce a microcin that induces the SOS response in target bacteria. Besides adding to the limited number of microcins known to be produced by *E. coli*, this study provides an additional mechanism by which *stx2a* expression is increased in response to the gut microflora.

Importance

How the gut microflora influences the progression of bacterial infections is only beginning to be understood. Antibiotics are counter-indicated for *E. coli* O157:H7 infections, and therefore treatment options are limited. An increased understanding of how the gut microflora directs O157:H7 virulence gene expression may lead to additional treatment options. This work identified *E. coli* that enhance the production of Shiga toxin by O157:H7, through the secretion

of a proposed microcin. This work demonstrates another mechanism by which non-O157 *E. coli* strains may increase Shiga toxin production, and adds to our understanding of microcins, a group of antimicrobials that are less well understood than colicins.

Introduction

E. coli O157:H7 is a notorious member of the enterohemorrhagic *E. coli* (EHEC) pathotype, which causes hemolytic colitis and hemolytic uremic syndrome (HUS) through production of virulence factors including the locus of enterocyte effacement (LEE) and Shiga toxins (Stx) (1, 2). Stx is encoded on a lambdoid prophage (3). Induction of the prophage and subsequent upregulation of *stx* is tied to activation of the bacterial SOS response (4). Therefore, DNA damaging agents including certain antibiotics increase Stx synthesis, and are typically counter indicated during treatment (5). There are two Stx types, referred to as Stx1 and Stx2 (6). Stx1 is further divided into three subtypes, Stx1a, Stx1c and Stx1d (7). Stx2 also has multiple subtypes, designated Stx2a, Stx2b, Stx2c, Stx2d, Stx2e, Stx2f, Stx2g (7), Stx2h (8) and Stx2i (9). In general, infections caused by Stx1, and interestingly, even those with both Stx1 and Stx2 (such as strains EDL933 (10) and Sakai (11)) are associated with less severe disease symptoms than Stx2-only producing *E. coli* (12–14). Of the Stx2 subtypes, Stx2a is more commonly associated with clinical cases and instances of HUS (14–17). Indeed, the FAO and WHO considers STEC carrying *stx2a* to be of greatest concern (18).

Stx2a levels can be affected *in vitro* and *in vivo* when *E. coli* O157:H7 is cultured along with other bacteria. Indeed, it was found that *stx2a* expression is downregulated by various probiotic species (19, 20) or in a media conditioned with human microbiota (21). Conversely, non-pathogenic *E. coli* that are susceptible to infection by the *stx2a*-converting phage were

reported to increase Stx2a levels (22, 23). This mechanism is O157:H7 strain-dependent (23), and requires expression of the *E. coli* BamA, which is the phage receptor (24, 25).

Production of Stx2a by O157:H7 can also increase in response to molecules secreted by other members of the gut microbiota (24, 26), such as bacteriocins and microcins. Bacteriocins are proteinaceous toxins produced by bacteria that inhibit the growth of closely related bacteria. For example, a colicin E9 (ColE9) producing strain amplified Stx2a when grown together with Sakai to higher levels than a colicin E3 (ColE3) producing strain (26). ColE9 is a DNase, while ColE3 has RNase activity, and this may explain the differences in SOS induction and Stx2a levels. In support of this, the addition of extracted DNase colicins to various *E. coli* O157:H7 strains increased Stx2a production, but not Stx1 (26). Additionally, microcin B17 (MccB17), a DNA gyrase inhibitor, was shown to amplify Stx2a production (24).

This work is part of a continuing effort to identify mechanisms by which members of the gut microbiome, especially *E. coli*, enhance Stx2a production of *E. coli* O157:H7. Of particular interest was the identification of secreted enhancer molecules, which were not investigated in our earlier studies. It was hypothesized that non-pathogenic *E. coli* strains could secrete additional colicins and microcins capable of increasing Stx2a production by O157:H7.

Results

0.1229 amplifies Stx2a production in a cell independent manner

Human-associated *E. coli* isolates were tested for their ability to enhance Stx2a production in co-culture with O157:H7. Strain 0.1229 significantly increased Stx2a production of PA2, compared to PA2 alone (Fig. 1). C600 was included as a positive control, as it was previously shown to increase Stx2a production when co-cultured with O157:H7 (22, 23).

Growth of PA2 in cell-free supernatants of 0.1229 also amplified Stx2a production, indicating this phenomenon does not require whole cells (Fig. 2A). Sequencing of the genome of 0.1229 using Illumina technology revealed that it belonged to the same sequence type (ST73) as *E. coli* strains CFT073 (27) and Nissle 1917 (28), and carried a plasmid similar to pRS218 in *E. coli* RS218 (29). However, supernatants harvested after growth of these strains failed to increase Stx2a production by PA2 (Fig. 2A). To test whether increased Stx2a production was dependent on *recA*, 0.1229 was co-cultured with the W3110Δ*tolC* P*recA-gfp* reporter strain. As anticipated, we found that among this collection, only strain 0.1229 increased GFP expression as a co-culture (Fig. 2B). Treatment of 0.1229 supernatants revealed this bioactivity was resistant to boiling, and sensitive to Proteinase K (Fig. 2C).

The plasmids of 0.1229 may play a role in Stx2a amplification

Further analysis of the Illumina sequence data revealed high sequence identity between the chromosomes of 0.1229, CFT073, Nissle 1917 and RS218 (data not shown). The most notable differences were in predicted plasmid content. To obtain a more complete picture, PacBio long read technology was used to sequence the genome of 0.1229.

The largest plasmid of 0.1229, designated p0.1229_1, was 114,229 bp, and 99.99% identical with 100% query coverage to pUTI89 (30) and pRS218 (29) (Fig. 3A). A second plasmid designated p0.1229_2 had five identifiable antimicrobial resistance genes, was 96,272 bp, and encoded the operon for microcin B17 (MccB17), a microcin that inhibits DNA gyrase (31). The plasmid p0.1229_2 shared high sequence identity with other known plasmids, being 99.96% identical with 57% query to pRS218, 97.81% identical with 82% query to pECO-fce (NCBI accession CP015160) and 100% identical with 89% query to pSF-173-1 (32) (Fig. 3B). A third plasmid was smaller than the cutoff for size selection used during PacBio library

115 preparation but was closed by Illumina sequencing. This plasmid, designated p0.1229_3, was
116 12,894 bp and encoded ampicillin resistance (*blaTEM-1b*) (Fig. 3C). It was similar to pEC16II
117 (NCBI accession KU932034), 99.85% identical with 61% query, and to pHUSEC41-3 (33),
118 98.89% identical with 61% query.

119 As RS218 did not amplify Stx2a production (Fig. 2A), it was assumed that p0.1229_1 did
120 not encode the genes responsible for this phenotype. Similarly, *E. coli* strain SF-173 did not
121 increase GFP when co-cultured with W3110Δ*tolC* P*recA-gfp,* suggesting genes encoded on
122 p0.1229_2 were also not required (data not shown).

123 **Strain 0.1229 encodes microcin B17, which is partially responsible for Stx2a amplification**

124 Microcin B17 (MccB17) is a 3.1 kDa (43 amino acid) DNA gyrase inhibitor that is found
125 on a seven gene operon, with *mcbA* encoding the 69 amino acid microcin precursor (31).
126 Although pSF-173-1 encodes this operon, there was a three-nucleotide deletion observed in
127 *mcbA* in pSF-173-1, compared to an earlier published sequence (31). This deletion is predicted to
128 shorten a ten Gly homopolymeric stretch by one amino acid residue. Although this Gly rich
129 region is not important for interaction with the gyrase-DNA complex (34), it seemed prudent to
130 confirm that the results reported above with strain SF-173 were not due to production of a non-
131 functional McbA. Therefore, knockouts of *mcbA* (Δ*mcbA*), and the entire operon
132 (Δ*mcbABCDEFG*) were constructed in 0.1229. These mutations decreased Stx2a amplification
133 by O157:H7 compared to wildtype 0.1229 (Fig. 4A) however they did not ablate the Stx2a levels
134 back to mono-culture levels. Similar results were seen with the P*recA-gfp* strain (Fig. 4B),
135 although differences were less pronounced than those seen with the Stx assays.

136 **Four ORFs encoded by p0.1229_3 are necessary for Stx2a amplification phenotype**

It was next hypothesized that p0.1229_3 encoded the activity responsible for Stx2a amplification by 0.1229Δ*mcbA* and 0.1229Δ*mcbABCDEFG.* A C600 strain transformed with p0.1229_3 amplified Stx2a production of PA2 (Fig. 5), confirming the importance of this plasmid. By systematically deleting portions of p0.1229_3, two regions were identified as essential for increased Stx2a production (Fig. 6A). The genes annotated in these regions are referred to as hypothetic proteins (hp), domains of unknown (DUF), an ATP-binding cassette (ABC)-type transporter and a member of the cupin superfamily of conserved barrel domains. The mutant, 0.1229 Δ6 (2850-5473 bp), deleted two open reading frames (ORFs), referred to as *hp1* and *ABC*, and 0.1229 Δ7 (5426-7950 bp) deleted *cupin*, *DUF4440*, *DUF2164*, *hp2*, *hp3* and a portion of a nuclease (Fig. 6B). These results were confirmed using co-culture assays with the P*recA-gfp* reporter (Fig. S1). Insertional inactivation of individual ORFs in these regions identified four, *hp1*, *abc*, *cupin,* and *hp2*, that were necessary for enhanced Stx2a production (Fig. 6C). Similar results were shown in co-culture with P*recA-gfp*, although 0.1229Δ*hp2* showed only a moderate decrease in GFP expression (Fig. S1). Cloning of a 5.2kb region of the plasmid, spanning upstream of *hp1* through the beginning of the putative nuclease-encoding gene, confirmed this activity is encoded within this region (Fig. 6D). Cloning of a similar region that ended after *abc* did not provide C600 the ability to increase GFP (data not shown).

In silico comparisons identified a nearly identical gene cluster in other species, including *Shigella sonnei* and *Klebsiella pneuomoniae* (Fig. S2). The region of p0.1229_3 spanning nucleotides 2745 to 7238bp was greater than 99.6% identical on the nucleotide level, when comparing all the strains in Fig. S2. Similar gene clusters containing Hp1 at 36 to 68% amino acid identity, were found in other species as well (Fig. S3). In these clusters, orthologs to *hp1*, *abc*, and *cupin* were commonly co-localized and the genes were found in the same order.

160 **The secreted molecule requires *tolC* for secretion, and *tonB* for import into target strains**

161 Some bacteriocins and microcins require genes encoded outside of the main operon for
162 secretion, such as the efflux protein TolC (35). The supernatant of 0.1229Δ*tolC* did not increase
163 Stx2a expression by strain PA2 to levels seen with wildtype 0.1229 supernatants (data not
164 shown). Similar results were observed in co-culture experiments using the P*recA-gfp* carrying
165 strain (Fig. 8). The phenotype was restored when *tolC* was complemented on a plasmid, but only
166 when tested with the P*recA-gfp* strain (Fig. 7). Similarly, numerous bacteriocins are translocated
167 into target cells using the TonB system (36). A *tonB* knockout was constructed in the P*recA-gfp*
168 reporter strain, as we were unsuccessful generating this in a O157:H7 background. In co-culture
169 with 0.1229, the MG1655Δ*tonB* P*recA-gfp* strain produced lower GFP levels than the MG1655
170 P*recA-gfp* strain (Fig. 8). This phenotype was restored when pBAD24::*tonB*, but not pBAD24,
171 was transformed into the mutant strain (Fig. 8).

172 **The gene cluster was identified in additional strains**

173 Lastly, it was hypothesized that *E. coli* isolated from human feces would encode the
174 similar molecules identified here. A total of 101 human fecal *E. coli* isolates were obtained from
175 Penn State's *E. coli* Reference Center, and three of these were found to induce GFP production
176 in the P*recA-gfp* reporter assay (Fig. S4). Furthermore, the supernatants of two of these isolates,
177 designated 91.0593 and 99.0750, increased Stx2a to levels similar to 0.1229, however 90.2723
178 did not (Fig. 9A). Genome sequencing of these three organisms revealed that 91.0593 and
179 99.0750 carried plasmids similar to p0.1229_3, however the latter plasmid had a deletion in the
180 recombinase and transposon regions (Fig. 9B). Strain 99.0750 was molecular serotype O36:H39,
181 while 91.0593 could not be O typed but was identified as H10.

182
183

Discussion

The concentration of *E. coli* in human feces ranges from 10^7 to 10^9 colony forming units (CFU) (37, 38). Typically, there are up to five commensal *E. coli* strains colonizing the human gut at a given time (39, 40). As the human microbiota affects O157:H7 colonization and virulence gene expression (41–44), it is thought that community differences in the gut microflora may explain, in part, individual differences in disease symptoms (45). Indeed, commensal *E. coli* that are susceptible to *stx2*-converting phage can increase phage and Stx production (22, 23). In mice given a co-culture of O157:H7 and phage-resistant *E. coli*, minimal toxin was recovered in the feces, but with *E. coli* that were phage-susceptible, higher levels of toxin were found (46). However, it is clear that phage infection of susceptible bacteria is not the only mechanism by which the gut microflora affects Stx2 levels during infection (19, 20, 24, 26).

In this study, both whole cells and spent supernatants of *E. coli* 0.1229 enhanced Stx2a production by *E. coli* O157:H7 strain PA2. This latter strain is a member of the hypervirulent clade 8 (47) and was previously found to be a high Stx2a producer in co-culture with *E. coli* C600 (23). *E. coli* 0.1229 produces at least two molecules capable of increasing Stx2a. The first is MccB17, a DNA gyrase inhibitor, shown to activate Stx2a production in an earlier study (24). This current study identified a second molecule localized to a 12.8 kb plasmid, and all genes necessary for production are found within a 5.2 kb region. Furthermore, gene knockouts identified four potential ORFs within this region, *hp1*, *abc*, *cupin* and *hp2*, that are required for 0.1229 mediated Stx2a amplification. This gene cluster was also identified on pB51 (48), a similar plasmid to p0.1229_3, however limited characterization was reported.

Oxidizing agents, such as hydrogen peroxide (H_2O_2), and antibiotics targeting DNA replication, such as ciprofloxacin, mitomycin C and norfloxacin, are known to induce *stx*-

207 converting phage (5, 49, 50) and subsequently Stx2 production (5, 49). However, the Stx2
208 amplifying activity of the 0.1229 supernatant was abolished by Proteinase K, suggesting the
209 inducing molecule is proteinaceous in nature. Colicins are bacteriocins found in *E. coli* (51), are
210 generally greater than 30 kDa in size, and at least one member has been previously shown to
211 enhance O157:H7 Stx2 production (26). While some colicins utilize TonB for translocation, they
212 are not expected to be heat stable. The molecule produced by 0.1229 was resistant to 100°C for
213 10 minutes, strongly suggesting it is not a colicin.

214 Microcins are bacteriocins that are generally smaller than 10 kDa. Their size and lack of
215 secondary and tertiary structure make them more heat stable than colicins. Microcins are divided
216 into three classes; class I and class IIa are plasmid encoded, while class IIb are chromosomally
217 encoded. Class I and IIb are post-translationally modified (52, 53), while class IIa are not. To
218 date, all class II but only one member of class I (microcin J25) use an ATP-binding cassette
219 (ABC)-type transporter in complex with TolC for export (35), and the TonB system for import
220 into target cells (36). The putative microcin produced by 0.1229 is plasmid encoded, along with a
221 predicted ABC transporter and is TolC and TonB dependent. Therefore, this microcin appears to
222 be more closely related to class IIa microcins. However, purification of the microcin to identify
223 possible post translational modifications is necessary to confirm whether designating as class I or
224 IIa is more appropriate.

225 There are four known class IIa microcins, microcin V (MccV, previously named colicin
226 V) (54, 55), microcin N (MccN, previously named Mcc24) (56), microcin L (MccL) (57), and
227 microcin PDI (MccPDI) (58, 59). The operons encoding these microcins contain four or five
228 genes, including the microcin precursor, immunity and export genes. MccN also encodes a
229 putative regulator, with a histone-like nucleoid domain (56). The microcin precursor genes

possess leader sequences of approximately 15 amino acids, containing the signature sequence MRXI/LX(9)GG/A (X=any amino acid), and are typically cleaved by the ABC transporters during export (60). A potential leader sequence with the double glycine was found in *hp2*. Additionally, a small peptide (DHGSR) was identified in the supernatants of 0.1229 by mass spectroscopy (data not shown) corresponding to an ORF internal to *hp2* encoded in the opposite direction. Future experiments will determine if one of these, or another region, encodes a secreted microcin.

One argument against designation as a class IIa microcin, is the lack of an identifiable N-terminal proteolytic domain (61) in the predicted ABC transporter encoded on p0.1229_3. This domain is found in all other members of class IIa. Interestingly, the class I microcin J25 (MccJ25) also encodes an ABC transporter lacking this domain. Unlike the other class I microcins, MccJ25 is TolC and TonB dependent for export and import, respectively. While the possibility cannot be excluded that the system identified here is a class I microcin, if so, it is more similar to MccJ25 than to other members of this group.

While the current mechanism of action is unknown, it is theorized that the putative microcin causes DNA damage, through double strand breaks, depurination, or inhibition of DNA replication. Such actions would lead to RecA-dependent phage induction and Stx2 production. The suspected mode of action would be divergent from the known class IIa microcins, which target the inner membrane (62) and MccJ25 which inhibits the RNA polymerase (63). Besides the predicted ABC transporter, the functions of the other ORFs is unclear. We anticipate one of these may encode an ABC accessory protein, known to be essential for these export complexes (64). One ORF encodes a cupin domain found in a functionally diverse set of proteins. An immunity gene protecting the host may also be expected in this region.

253 The genes encoding the putative microcin were additionally found in *E. coli* strains
254 99.0750 and 91.0593. Genome sequencing of these strains failed to identify genes encoding
255 MccB17, which may explain the lower levels of Stx2a production seen in co-culture with PA2
256 compared to those seen with 0.1229. Bioinformatic analyses also identified other *E. coli* that
257 encode nearly identical regions. Interestingly, one of these was *E. coli* O104:H4 HUS, isolated in
258 2001 (33), and responsible for a large 2011 outbreak in Germany. However, a premature stop
259 codon identified in *cupin* suggests it is non-functional. Homologs of *hp1*, *ABC* and *cupin* were
260 identified together in several other organisms distantly related to *E. coli,* suggesting these encode
261 a functional unit. The absence of *hp2* in most of these genetic clusters argues against this ORF
262 encoding the anti-bacterial activity or may suggest that these organisms encode microcins
263 distinct from *hp2*.
264 In conclusion, a putative microcin was identified in *E. coli*, expanding our knowledge of
265 this small group of antimicrobial peptides. This study also identifies another mechanism by
266 which *E. coli* may enhance Stx2a production by *E. coli* O157:H7. Further studies may also
267 provide new insights into the diverse genetic structure and functions of microcin-encoding
268 systems.
269

270 **Materials & Methods**

271 **Bacterial strains, media and growth conditions**

272 *E. coli* strains were grown in Lysogeny Broth (LB) at 37°C unless otherwise indicated,
273 and culture stocks were maintained in 20% glycerol at −80°C. Antibiotics were used at the
274 following concentrations; ampicillin (100 μg/ml), chloramphenicol (25 μg/ml), kanamycin (50
275 μg/ml), and tetracycline (10 μg/ml). All bacterial isolates, plasmids and primers used in this

study can be found in Table 1. *E. coli* SF-173-1 was provided by Dr. Craig Stephens, Santa Clara University.

Co-culture with PA2

Co-culture with *E. coli* O157:H7 PA2 was performed similar to previously described (23). PA2 and commensal *E. coli* strains were grown overnight at 37°C (with shaking at 250 rpm). LB agar (2.5 ml) was added to 6-well plates (BD Biosciences Inc., Franklin Lakes, NJ), and allowed to solidify. PA2 and commensal strains were each diluted to an OD_{600} of 0.05 in 1 ml of LB broth and added to the 6-well plates. A mono-culture of PA2 (at 0.05 OD_{600} in 1ml) served as a negative control. The plates were incubated without shaking at 37°C. After 16 hr, cultures were collected, cells were lysed with 6 mg/ml polymyxin B at 37°C for 5 min, and supernatants were collected. Samples were immediately tested with the receptor-based enzyme-linked immunosorbent assay (R-ELISA), as described below, or stored at -80°C. Total protein was calculated using the Bradford assay (VMR Life Science, Philadelphia, PA), and used to calculate μg/mg Stx2.

R-ELISA for Stx2a detection

Detection of Shiga toxin was performed using a sandwich ELISA approach, previously described by Xiaoli *et al*., 2018 (24). Briefly, 25 μg/ml of ceramide trihexosides (bottom spot) (Matreya Biosciences, Pleasant Gap, PA) dissolved in methanol was used for coating of the plate. Washes were performed between each step using PBS and 0.05% Tween-20. Stx2a-containing samples were diluted in PBS as necessary to obtain final readings in the linear range. Samples were added to the wells in duplicate and incubated with shaking for 1 hr at room temperature. Supernatants of *E. coli* PA11, a high Stx2a producer (65), were used as a positive control. Anti-Stx2 monoclonal mouse antibody (Santa Cruz Biotech, Santa Cruz CA) was added

to the plate at a concentration of 1 μg/ml, then incubated for 1 hr. Anti-mouse secondary antibody (MilliporeSigma, Burlington MA) conjugated to horseradish peroxidase (1 μg/ml) was added to the plate, and incubated for 1 hr. For detection, 1 step Ultra-TMB (Thermo-Fischer, Waltham, MA) was used, and 2M H_2SO_4 was added to the wells to stop the reaction. The plate was read at 450 nm using a DU®730 spectrophotometer (Beckman Coulter, Atlanta, GA). A standard curve was generated from two-fold serially diluted PA11 samples and used to quantify the μg/ml of Stx2a present in each sample.

Cell-free supernatant assay with PA2

E. coli O157:H7 strain PA2 and non-pathogenic *E. coli* strains were individually grown with shaking at 37°C for 16 hr. Overnight culture of the non-pathogenic strains were centrifuged, and supernatants were filtered through 0.2 μm cellulose filters (VWR International, Radnor, PA). LB agar (2.5 ml) was added to the wells of 6-well plates (BD Biosciences Inc., Franklin Lakes, NJ) and allowed to solidify. PA2 was added to wells at a final density of 0.05 OD_{600} in 1 ml of spent supernatant. For the negative control, PA2 was resuspended in fresh LB broth to the same cell density, and 1 ml was added to a well. The plates were statically incubated at 37°C for 8 hr, after which the cell density (OD_{600}) was recorded. Cells were lysed with 6 mg/ml Polymyxin B at 37°C for 5 min and supernatant recovered. Samples were immediately tested for Stx2a by R-ELISA or stored at -80°C. Data reported as μg/ml/OD_{600}.

Detection of SOS inducing agents using P*recA-gfp*

E. coli expressing P*recA-gfp*, which encodes green fluorescent protein (*gfp*) under control of the *recA* promoter (66), was purchased from Dharmacon (Lafayette, CO). The plasmid was transformed into *E. coli* W3110Δ*tolC*. The *tolC* deletion reduces the potential efflux of *recA*-activating molecules. W3110Δ*tolC* P*recA-gfp* and commensal strains were individually grown

overnight with shaking at 37°C. LB agar (2.5 ml) was added to 6-well plates and allowed to solidify. W3110Δ*tolC* P*recA-gfp* and one commensal strain were each diluted to a final OD_{600} of 0.05 in LB broth, and 1ml was added to the 6-well plates. The negative control included only W3110Δ*tolC* P*recA-gfp* at a final OD of 0.05 in 1 ml LB broth. The plates were statically incubated at 37°C. After 16 hr, 100 µl was removed from each well, added to black 96 well clear bottom plates (Dot Scientific Inc., Burton, MI) and optical density (OD_{620}) was read using a DU®730 spectrophotometer. Relative fluorescence units (RFU) were measured at an excitation of 485 nm and emission of 538 nm on a Fluoroskan Ascent FL (Thermo Fisher Scientific, Waltham, MA) (67). RFU values were normalized to cell density.

One step recombination for *E. coli* knockouts

Mutants of 0.1229 and MG1655 were constructed using one-step recombination (68). Primers contained either 50 bp upstream or downstream of the gene of interest, followed by sequences annealing to the P1 and P2 priming sites from pKD3. PCR was performed at the following settings: initial denaturation at 95°C for 30s; 10 cycles of 95°C 30s, 49°C 60s, 68°C 100s; 24 cycles of 95°C 30s, T_a 60s, 68° at variable time, and a final extension at 68°C for 5min. T_a and variable times for each set of primers are reported in Table 1. A derivative of pKD46-Kan^R was used as 0.1229 is resistant to Amp^R. Electroporation was used to construct *E. coli* 0.1229(pKD46) and MG1655(pKD46), using a Bio-Rad Gene Pulser II and following protocols recommended by the manufacturer. Colonies containing pKD46-Kan^R were selected on LB plates with kanamycin. Strains containing pKD46 were grown to an OD_{600} of 0.3, and L-arabinose was added to a final concentration of 0.2M. After incubation for 1 hr, cells were washed and electroporated with the pKD3-derived PCR product. Transformants were selected on LB plates with chloramphenicol. Knockouts were confirmed by PCR using primers ~200bp

upstream and downstream of the gene, using standard PCR settings (initial denaturation at 95°C for 30s; 35 cycles of 95°C 30s, variable amplification temperature (T_a) 60s, 68°C at variable time; and a final extension at 68°C for 5min). This strategy was followed for all the knockouts, including primers and temperatures specific for each gene (Table 1).

Gibson cloning

The 2745-7950 bp region of p0.1229_3 was cloned into pBR322 (pBR322::p0.1229_3$^{2745\text{-}7950}$), using Gibson cloning as previously described (69). Briefly, primer pairs were constructed containing 30 bp annealing to the pBR322 insert site and 30 bp that would anneal to p0.1229_3. DNA from 0.1229 and pBR322 was amplified at these sites using standard PCR settings, amplicons were cleaned up using a PCR purification kit (Qiagen, Germantown, MD) and subjected to assembly at 50°C using the Gibson cloning kit (New England Biosciences, Ipswich, MA). Assembled plasmids were propagated in DH5α competent cells (New England Biosciences, Ipswich, MA). Verification PCR was performed using primers 200 bp upstream and downstream of the insert site (Table 1) and confirmed using Sanger sequencing. Successful constructs were transformed into C600 electrocompetent cells. A similar process was used to clone *tolC* in pBAD18 (Kan^R).

Whole genome sequencing and bioinformatics

For the whole genome sequencing of 0.1229, genomic DNA was isolated using the Wizard Genomic DNA purification kit (Promega, Madison, WI). Whole genome sequencing was performed at the Penn State Genomics Core facility using the Illumina MiSeq platform. A PCR-free DNA kit was used for library preparation. The sequencing run produced 2 x 150 bp reads.

For the whole genome sequencing of 99.0750, 91.0593, and 90.2723, genomic DNA was isolated using Qiagen DNeasy Blood and Tissue Kit (Qiagen Inc., Germantown, MD). Whole

genome sequencing was performed using the NexTera XT DNA library prep kit and run on an Illumina MiSeq platform. The sequencing run produced 2 x 250 bp reads.

After Illumina sequencing, Fastq files were checked using Fastqc v0.11.5 (70) and assembled using SPAdes v3.10 (71). SPAdes assemblies were subjected to the Quality Assessment Tool for Genome Assemblies v4.5 (QUAST) (72), and contig number, genome size, N50 and GC % were noted.

Strain 0.1229 was also sequenced at the Center for Food Safety and Nutrition, Food and Drug Administration using the Pacific Biosciences (PacBio) RS II sequencing platform, as previously reported (73). For library preparation, 10 µg genomic DNA was sheared to 20 kb fragments by g-tubes (Covaris, Inc., Woburn, MA, USA) according to the manufacturer's instructions. The SMRTbell 20 kb template library was constructed using DNA Template Prep kit 1.0 (Pacific Biosciences, Menlo Park, CA, USA). BluePippin (Sage Science, Beverly, MA, USA) was used for size selection, and sequencing was performed using the P6/C4 chemistry on two single-molecule real-time (SMRT) cells with a 240 min collection protocol along with stage start. SMRT Analysis 2.3.0 was used for read analysis, and de novo assembly using the PacBio Hierarchical Genome Assembly Process (HGAP3.0) program. The assembly output from HGAP contained overlapping regions at the end which can be identified using dot plots in Gepard (74). The genome was checked manually for even sequencing coverage. Afterwards, the improved consensus sequence was uploaded in SMRT Analysis 2.3.0 to determine the final consensus and accuracy scores using Quiver consensus algorithm (75). The assembled genome was annotated using the NCBI's Prokaryotic Genomes Automatic Annotation Pipeline (PGAAP) (76).

Plasmid sequences were visualized using Blast Ring Image Generator v0.95 (BRIG) (77). The Center for Genomic Epidemiology website was used for ResFinder v3.1.0 (90% identity,

60% length) (78), SerotypeFinder v2.0.1 (85% identity, 60% length) (79) and MLSTFinder v2.0.1 (80) using the Achtman multi-locus sequence typing (MLST) scheme (81). The Integrated Microbial Genomics & Microbiomes website of DOE's Joint Genome Institute was utilized to BLAST the amino acid sequence of Hp1 against other genomes, matches that were between 36 and 68% identical from varying species were selected, then visualized using the gene neighborhoods function (82).

Data Analysis

MS Excel (Microsoft Corporation, Albuquerque NM) was used to calculate the mean, standard deviation, and standard error; and GraphPad Prism 6 (GraphPad Software, San Diego CA) was used for generating figures. Error bars report standard error of the mean from at least three biological replicates.

Data availability

Nucleotide and SRA files for the 0.1229 can be found on NCBI under Biosample SAMN08737532. SRA files for 99.0750 (SAMN11457477), 91.0593 (SAMN11457478), 90.2723 (SAMN11457479) can be found under their respective accession numbers.

Acknowledgements

We thank Dr. Craig Stephens at Santa Clara University for providing strain SF-173, Dr. Roberto Kolter at Harvard Medical School for providing strain ZK1526, and Erin Nawrocki for manuscript proofreading. HF was supported by USDA National Needs Grant 2014-38420-21822. This work was supported by grant number 1 R21 AI130856-01A1 through the National Institute of Allergy and Infectious Diseases and the USDA National Institute of Food and Agriculture Federal Appropriations under project PEN04522 and accession number 0233376.

References

1. Griffin PM, Tauxe R V. 1991. The Epidemiology of Infections Caused by *Escherichia coli* O157:H7, Other Enterohemorrhagic *E. coli*, and the Associated Hemolytic Uremic Syndrome. Epidemiol Rev 13:60–98.
2. Nguyen Y, Sperandio V, Padola NL, Starai VJ. 2012. Enterohemorrhagic *E. coli* (EHEC) pathogenesis. Front Cell Infect Microbiol 2:1–7.
3. Hayashi T, Makino K, Ohnishi M, Kurokawa K, Ishii K, Yokoyama K, Han C-G, Ohtsubo E, Nakayama K, Murata T, Tanaka M, Tobe T, Iida T, Takami H, Honda T, Sasakawa C, Ogasawara N, Yasunaga T, Kuhara S, Shiba T, Hattori M, Shinagawa H. 2001. Complete Genome Sequence of Enterohemorrhagic *Eschelichia coli* O157:H7 and Genomic Comparison with a Laboratory Strain K-12. DNA Res 8:11–22.
4. Waldor MK, Friedman DI. 2005. Phage Regulatory Circuits and Virulence Gene Expression. Curr Opin Microbiol 8:459–465.
5. Zhang X, McDaniel AD, Wolf LE, Keusch GT, Waldor MK, Acheson DW. 2000. Quinolone Antibiotics induce Shiga toxin-encoding Bacteriophages, Toxin production, and Death in Mice. J Infect Dis 181:664–670.
6. Scotland S, Smith HR, Rowe B. 1985. Two Distinct Toxins active on Vero cells from *Escherichia coli* O157. Lancet 2:885–886.
7. Scheutz F, Teel LD, Beutin L, Piérard D, Buvens G, Karch H, Mellmann A, Caprioli A, Tozzoli R, Morabito S, Strockbine NA, Melton-Celsa AR, Sanchez M, Persson S, O'Brien AD. 2012. Multicenter Evaluation of a Sequence-based Protocol for Subtyping Shiga toxins and Standardizing Stx Nomenclature. J Clin Microbiol 50:2951–2963.

437 8. Bai X, Fu S, Zhang J, Fan R, Xu Y, Sun H, He X, Xu J, Xiong Y. 2018. Identification and
438 Pathogenomic Analysis of an *Escherichia coli* Strain Producing a Novel Shiga toxin 2
439 Subtype. Sci Rep 8:1–11.
440 9. FAO/WHO STEC Expert Group. 2018. Hazard Identification and Characterization:
441 Criteria for Categorizing Shiga Toxin–Producing *Escherichia coli* on a Risk Basis. J Food
442 Prot 82:7–21.
443 10. Strockbine NA, Marques LR, Newland JW, Smith HW, Holmes RK, O'Brien AD. 1986.
444 Two toxin-converting Phages from *Escherichia coli* O157:H7 strain 933 encode
445 Antigenically Distinct Toxins with Similar Biologic Activities. Infect Immun 53:135–140.
446 11. Matsushiro A, Sato K, Miyamoto H, Yamamura T, Honda T. 1999. Induction of
447 Prophages of Enterohemorrhagic *Escherichia coli* O157:H7 with Norfloxacin. J Bacteriol
448 181:2257–2260.
449 12. Ostroff S, Tarr P, Neill MA, Lewi JH, Hargrett-Bean N, Ostroff S, Tarr P, Neill MA, Lewi
450 JH, Kobayashi JM. 1989. Toxin Genotypes and Plasmid Profiles as Determinants of
451 Systemic Sequelae in *Escherichia coli* 0157:H7 Infections. J Infect Dis 160:994–998.
452 13. Donohue-Rolfe A, Kondova I, Oswald S, Hutto D, Tzipori S. 2000. *Escherichia coli*
453 O157:H7 Strains That Express Shiga Toxin (Stx) 2 Alone Are More Neurotropic for
454 Gnotobiotic Piglets Than Are Isotypes Producing Only Stx1 or Both Stx1 and Stx2. J
455 Infect Dis 181:1825–1829.
456 14. Orth D, Grif K, Khan AB, Naim A, Dierich MP, Würzner R. 2007. The Shiga toxin
457 Genotype Rather than the Amount of Shiga toxin or the Cytotoxicity of Shiga toxin *in*
458 *vitro* Correlates with the Appearance of the Hemolytic Uremic Syndrome. Diagn
459 Microbiol Infect Dis 59:235–242.

15. Persson S, Olsen KEP, Ethelberg S, Scheutz F. 2007. Subtyping Method for *Escherichia coli* Shiga Toxin (Verocytotoxin) 2 Variants and Correlations to Clinical Manifestations. J Clin Microbiol 45:2020–2024.

16. Shringi S, Schmidt C, Katherine K, Brayton KA, Hancock DD, Besser TE. 2012. Carriage of *stx2a* Differentiates Clinical and Bovine-Biased Strains of *Escherichia coli* O157. PLoS One 7:e51572.

17. Kawano K, Okada M, Haga T, Maeda K, Goto Y. 2008. Relationship between Pathogenicity for Humans and *stx* Genotype in Shiga toxin-Producing *Escherichia coli* Serotype O157. Eur J Clin Microbiol Infect Dis 27:227–232.

18. FAO/WHO. 2018. Shiga toxin-producing *Escherichia coli* (STEC) and Food: Attribution, Characterization, and Monitoring. Rome.

19. Carey CM, Kostrzynska M, Ojha S, Thompson S. 2008. The Effect of Probiotics and Organic Acids on Shiga-toxin 2 Gene Expression in Enterohemorrhagic *Escherichia coli* O157:H7. J Microbiol Methods 73:125–132.

20. Thévenot J, Cordonnier C, Rougeron A, Le Goff O, Nguyen HTT, Denis S, Alric M, Livrelli V, Blanquet-Diot S. 2015. Enterohemorrhagic *Escherichia coli* Infection has Donor-dependent Effect on Human Gut Microbiota and May be Antagonized by Probiotic Yeast during Interaction with Peyer's Patches. Appl Microb Cell Physiol 99:9097–9110.

21. de Sablet T, Chassard C, Bernalier-Donadille A, Vareille M, Gobert AP, Martin C. 2009. Human Microbiota-Secreted Factors Inhibit Shiga Toxin synthesis by Enterohemorrhagic *Escherichia coli* O157:H7. Infect Immun 77:783–790.

22. Gamage SD, Strasser JE, Chalk CL, Weiss AA. 2003. Nonpathogenic *Escherichia coli* Can Contribute to the Production of Shiga Toxin. Infect Immun 71:3107–3115.

483 23. Goswami K, Chen C, Xiaoli L, Eaton KA, Dudley EG. 2015. Coculture of *Escherichia*
484 *coli* O157:H7 with a Nonpathogenic *E . coli* Strain Increases Toxin Production and
485 Virulence in a Germfree Mouse Model. Infect Immun 83:4185–4193.
486 24. Xiaoli L, Figler HM, Goswami K, Dudley EG. 2018. Nonpathogenic *E. coli* Enhance
487 Stx2a Production of *E. coli* O157:H7 through bamA-Dependent and Independent
488 Mechanisms. Front Microbiol 9:1–13.
489 25. Smith DL, James CE, Sergeant MJ, Yaxian Y, Saunders JR, McCarthy AJ, Allison HE.
490 2007. Short-tailed stx phages Exploit the Conserved YaeT Protein to Disseminate Shiga
491 Toxin Genes Among Enterobacteria. J Bacteriol 189:7223–7233.
492 26. Toshima H, Yoshimura A, Arikawa K, Hidaka A, Ogasawara J, Hase A, Masaki H,
493 Nishikawa Y. 2007. Enhancement of Shiga Toxin Production in Enterohemorrhagic
494 *Escherichia coli* Serotype O157:H7 by DNase Colicins. Appl Environ Microbiol
495 73:7582–7588.
496 27. Mobley HLT, Green DM, Trifillis AL, Johnson DE, Chippendale GR, Lockatell CV,
497 Jones BD, Warren JW. 1990. Pyelonephritogenic *Escherichia coli* and Killing of Cultured
498 Human Renal Proximal Tubular Epithelial Cells: Role of Hemolysin in Some Strains.
499 Infect Immun 58:1281–1289.
500 28. Nissle A. 1919. Weiteres über die Mutaflorbehandlung unter besonderer Berü
501 cksichtigung der chronischen Ruhr. Münchener Medizinische Wochenschrift 25:678–681.
502 29. Wijetunge DSS, Karunathilake KHEM, Chaudhari A, Katani R, Dudley EG, Kapur V,
503 DebRoy C, Kariyawasam S. 2014. Complete Nucleotide Sequence of pRS218, a Large
504 Virulence Plasmid, that Augments Pathogenic Potential of Meningitis-associated
505 *Escherichia coli* Strain RS218. BMC Microbiol 14:1–16.

506 30. Chen SL, Hung C-S, Xu J, Reigstad CS, Magrini V, Sabo A, Blasiar D, Bieri T, Meye RR,
507 Ozersky P, Armstrong JR, Fulton RS, Latreille JP, Spieth J, Hooton TM, Mardis ER,
508 Hultgren SJ, Gordon JI. 2006. Identification of Genes Subject to Positive Selection in
509 Uropathogenic Strains of *Escherichia coli*: A Comparative Genomics Approach. PNAS
510 103:5977–5982.
511 31. Davagnino J, Herrero M, Furlong D, Moreno F, Kolter R. 1986. The DNA Replication
512 Inhibitor Microcin B17 is a Forty-three-amino-acid Protein Containing Sixty Percent
513 Glycine. Proteins Struct Funct Genet 1:230–238.
514 32. Stephens CM, Skerker CM, Sekhon JM, Arkin MS, Riley AP. 2015. Complete Genome
515 Sequences of Four *Escherichia coli* ST95 Isolates from Bloodstream Infections. Genome
516 Announc 3:1241–1256.
517 33. Künne C, Billion A, Mshana SE, Schmiedel J, Domann E, Hossain H, Hain T,
518 Imirzalioglu C, Chakraborty T. 2011. Complete Sequences of Plasmids from the
519 Hemolytic-uremic Syndrome-associated *Escherichia coli* strain HUSEC41. J Bacteriol
520 194:532–533.
521 34. Thompson RE, Collin F, Maxwell A, Jolliffe KA, Payne RJ. 2014. Synthesis of Full
522 Length and Truncated Microcin B17 Analogues as DNA Gyrase Poisons. Org Biomol
523 Chem 12:1570–1578.
524 35. Delgado MA, Solbiati JO, Chiuchiolo MJ, Farías RN, Salomón RA. 1999. *Escherichia*
525 *coli* Outer Membrane Protein TolC is Involved in Production of the Peptide Antibiotic
526 Microcin J25. J Bacteriol 181:1968–1970.
527 36. Braun V, Patzer SI, Hantke K. 2002. Ton-dependent Colicins and Microcins: Modular
528 Design and Evolution. Biochimie 84:365–380.

529 37. Penders J, Thijs C, Vink C, Stelma FF, Snijders B, Kummeling I, van den Brandt PA,
530 Stobberingh EE. 2006. Factors Influencing the Composition of the Intestinal Microbiota in
531 Early Infancy. Pediatrics 118:511–521.
532 38. Slanetz LW, Bartley CH. 1957. Numbers of Enterococci in Water, Sewage, and Feces
533 determined by the Membrane Filter Technique with an improved medium. J Bacteriol
534 74:591–595.
535 39. Apperloo-renkema HZ, Van Der Waaij BD, Van Der Waaij D. 1990. Determination of
536 Colonization Resistance of the Digestive Tract by Biotyping of Enterobacteriaceae.
537 Epidemiol Infect 105:355–361.
538 40. Johnson JR, Owens K, Gajewski A, Clabots C. 2008. *Escherichia coli* Colonization
539 Patterns among Human Household Members and Pets, with Attention to Acute Urinary
540 Tract Infection. J Infect Dis 197:218–224.
541 41. Leatham MP, Banerjee S, Autieri SM, Conway T, Cohen PS, Mercado-lubo R. 2009.
542 Precolonized Human Commensal *Escherichia coli* Strains Serve as a Barrier to *E . coli*
543 O157 : H7 Growth in the Streptomycin-Treated Mouse Intestine. Infect Immun 77:2876–
544 2886.
545 42. Sperandio V, Mellies JL, Nguyen W, Shin S, Kaper JB. 1999. Quorum Sensing Controls
546 Expression of the Type III Secretion Gene Transcription and Protein Secretion in
547 Enterohemorrhagic and Enteropathogenic *Escherichia coli*. Proc Natl Acad Sci U S A
548 96:15196–15201.
549 43. Sperandio V, Torres AG, Gir N JA, Kaper JB. 2001. Quorum Sensing Is a Global
550 Regulatory Mechanism in Enterohemorrhagic *Escherichia coli* O157:H7. J Bacteriol
551 183:5187–5197.

552 44. Zhao T, Doyle MP, Harmon BG, Brown CA, Mueller PO, Parks AH. 1998. Reduction of
553 Carriage of Enterohemorrhagic *Escherichia coli* O157:H7 in Cattle by Inoculation with
554 Probiotic Bacteria. J Clin Microbiol 36:641–647.
555 45. Bell BP, Griffin PM, Lozano P, Christie DL, Kobayashi JM, Tarr PI. 1997. Predictors of
556 Hemolytic Uremic Syndrome in Children During a Large Outbreak of *Escherichia coli*
557 O157:H7 Infections. Pediatrics 100:1–6.
558 46. Gamage SD, Patton AK, Strasser JE, Chalk CL, Weiss AA. 2006. Commensal Bacteria
559 Influence *Escherichia coli* O157:H7 Persistence and Shiga toxin Production in the Mouse
560 Intestine. Infect Immun 74:1977–1983.
561 47. Amigo N, Mercado E, Bentancor A, Singh P, Vilte D, Gerhardt E, Zotta E, Ibarra C,
562 Manning SD, Larzábal M, Cataldi A. 2015. Clade 8 and Clade 6 Strains of *Escherichia*
563 *coli* O157:H7 from Cattle in Argentina have Hypervirulent-Like Phenotypes. PLoS One
564 10:e0127710.
565 48. Micenková L. 2016. PhD Thesis. Bacteriocinogeny in pathogenic and commensal
566 *Escherichia coli* strains. Masarykova Univerzita Lékařská Fakulta Biologický Ústav.
567 49. Bielaszewska M, Idelevich EA, Zhang W, Bauwens A, Schaumburg F, Mellmann A,
568 Peters G, Karch H. 2012. Effects of Antibiotics on Shiga toxin 2 Production and
569 Bacteriophage Induction by Epidemic *Escherichia coli* O104:H4 Strain. Antimicrob
570 Agents Chemother 56:3277–3282.
571 50. Łoś JM, Łoś M, Węgrzyn A, Węgrzyn G. 2010. Hydrogen Peroxide-mediated Induction
572 of the Shiga Toxin Converting Lambdoid Prophage ST2-8624 in *Escherichia coli*
573 O157:H7. FEMS Immunol Med Microbiol 58:322–329.
574 51. Cascales E, Buchanan SK, Duche D, Kleanthous C, Lloubes R, Postle K, Riley M, Slatin

S, Cavard D. 2007. Colicin Biology. Microbiol Mol Biol Rev 71:158–229.

52. Duquesne S, Destoumieux-Garzón D, Peduzzi J, Rebuffat S. 2007. Microcins, Gene-encoded Antibacterial Peptides from Enterobacteria. R Soc Chem 24:708–734.

53. Patzer SI, Baquero MR, Bravo D, Moreno F, Hantke K. 2003. The Colicin G, H and X Determinants Encode Microcins M and H47, which Might Utilize the Catecholate Siderophore Receptors FepA, Cir, Fiu and IroN. Microbiology 149:2557–2570.

54. Gilson L, Mahanty K, Kolter R. 1987. Four Plasmid Genes Are Required for Colicin V Synthesis, Export, and Immunity. J Bacteriol 169:2466–2470.

55. Chehade H, Braun V. 1988. Iron-regulated Synthesis and Uptake of Colicin V. FEMS Microbiol Lett 52:177–181.

56. Corsini G, Karahanian E, Tello M, Fernandez K, Rivero D, Saavedra JM, Ferrer A. 2010. Purification and Characterization of the Antimicrobial Peptide Microcin N. FEMS Microbiol Lett 312:119–125.

57. Morin N, Lanneluc I, Connil N, Cottenceau M, Pons AM, Sablé S. 2011. Mechanism of Bactericidal Activity of Microcin L in *Escherichia coli* and *Salmonella enterica*. Antimicrob Agents Chemother 55:997–1007.

58. Eberhart LJ, Deringer JR, Brayton K a., Sawant A a., Besser TE, Call DR. 2012. Characterization of a Novel Microcin that Kills Enterohemorrhagic *Escherichia coli* O157:H7 and O26. Appl Environ Microbiol 78:6592–6599.

59. Zhao Z, Orfe LH, Liu J, Lu S-Y, Besser TE, Call DR. 2017. Microcin PDI Regulation and Proteolytic Cleavage are Unique Among Known Microcins. Nat Publ Gr 7:1–14.

60. Havarstein LS, Holo H, Nes IF. 1994. The Leader Peptide of Colicin V Shares Consensus Sequences with Leader Peptides that are Common Among Peptide Bacteriocins Produced

by Gram-positive Bacteria. Microbiology 140:2383–2389.

61. Havarstein LS, Diep DB, Nes IF. 1995. A Family of Bacteriocin ABC transporters Carry out Proteolytic Processing of their Substrates Concomitant with Export. Mol Microbiol 16:229–240.

62. Yang CC, Konisky J. 1984. Colicin V-treated *Escherichia coli* Does Not Generate Membrane Potential. J Bacteriol 158:757–759.

63. Yuzenkova J, Delgado M, Nechaev S, Savalia D, Epshtein V, Artsimovitch I, Mooney RA, Landick R, Farias RN, Salomon R, Severinov K. 2002. Mutations of Bacterial RNA Polymerase Leading to Resistance to Microcin J25. J Biol Chem 277:50867–50875.

64. Gilson L, Mahanty HK, Kolter R. 1990. Genetic Analysis of an MDR-like Export System: The Secretion of Colicin V. EMBO J 9:3875–3884.

65. Hartzell A, Chen C, Lewis C, Liu K, Reynolds S, Dudley EG. 2011. *Escherichia coli* O157:H7 of Genotype Lineage-Specific Polymorphism Assay 211111 and Clade 8 Are Common Clinical Isolates Within Pennsylvania. Foodborne Pathog Dis 8:763–768.

66. Zaslaver A, Bren A, Ronen M, Itzkovitz S, Kikoin I, Shavit S, Liebermeister W, Surette MG, Alon U. 2006. A Comprehensive Library of Fluorescent Transcriptional Reporters for *Escherichia coli*. Nat Methods 3:623–628.

67. Fan J, de Jonge BLM, MacCormack K, Sriram S, McLaughlin RE, Plant H, Preston M, Fleming PR, Albert R, Foulk M, Mills SD. 2014. A Novel High-throughput Cell-based Assay Aimed at Identifying Inhibitors of DNA Metabolism in Bacteria. Antimicrob Agents Chemother 58:7264–7272.

68. Datsenko K, Wanner BL. 2000. One-step inactivation of chromosomal genes in *Escherichia coli* K-12 using PCR products. Proc Natl Acad Sci U S A 97:6640–6645.

69. Gibson DG, Young L, Chuang R-Y, Venter JC, Hutchison CA, Smith HO. 2009. Enzymatic Assembly of DNA Molecules up to Several Hundred Kilobases. Nat Methods 6:343–345.

70. Andrews S. 2010. FastQC: A Quality Control Tool for High Throughput Sequence Data. Babraham Bioinformatics. https://www.bioinformatics.babraham.ac.uk/projects/fastqc/

71. Bankevich A, Nurk S, Antipov D, Gurevich AA, Dvorkin M, Kulikov AS, Lesin VM, Nikolenko SI, Pham S, Prjibelski AD, Pyshkin A V., Sirotkin A V., Vyahhi N, Tesler G, Alekseyev MA, Pevzner PA. 2012. SPAdes: A New Genome Assembly Algorithm and Its Applications to Single-Cell Sequencing. J Comput Biol 19:455–477.

72. Gurevich A, Saveliev V, Vyahhi N, Tesler G. 2013. QUAST: Quality Assessment Tool for Genome Assemblies. Bioinformatics 29:1072–1075.

73. Yao K, Roberts RJ, Allard MW, Hoffmann M. 2017. Complete Genome and Methylome Sequences of *Salmonella enterica* subsp. *enterica* Serovars Typhimurium, Saintpaul, and Stanleyville from the SARA/SARB Collection. Genome Announc 5:e00031-17.

74. Krumsiek J, Arnold R, Rattei T. 2007. Gepard: A Rapid and Sensitive Tool for Creating Dotplots on Genome Scale. Bioinformatics 23:1026–1028.

75. Chin C-S, Alexander DH, Marks P, Klammer AA, Drake J, Heiner C, Clum A, Copeland A, Huddleston J, Eichler EE, Turner SW, Korlach J. 2013. Nonhybrid, Finished Microbial Genome Assemblies from Long-read SMRT Sequencing Data. Nat Methods 10:563–569.

76. Klimke W, Agarwala R, Badretdin A, Chetvernin S, Ciufo S, Fedorov B, Kiryutin B, O'Neill K, Resch W, Resenchuk S, Schafer S, Tolstoy I, Tatusova T. 2009. The National Center for Biotechnology Information's Protein Clusters Database. Nucleic Acids Res 37:D216–D223.

644 77. Alikhan N-F, Petty NK, Ben Zakour NL, Beatson SA. 2011. BLAST Ring Image
645 Generator (BRIG): Simple Prokaryote Genome Comparisons. BMC Genomics 12:1–10.
646 78. Zankari E, Hasman H, Cosentino S, Vestergaard M, Rasmussen S, Lund O, Aarestrup FM,
647 Larsen MV. 2012. Identification of Acquired Antimicrobial Resistance Genes. J
648 Antimicrob Chemother 67:2640–2644.
649 79. Joensen KG, Tetzschner AMM, Iguchi A, Aarestrup FM, Scheutz F. 2015. Rapid and
650 Easy In Silico Serotyping of *Escherichia coli* Isolates by Use of Whole-Genome
651 Sequencing Data. J Clin Microbiol 53:2410–2426.
652 80. Larsen M V, Cosentino S, Rasmussen S, Friis C, Hasman H, Marvig RL, Jelsbak L,
653 Sicheritz-Pontén T, Ussery DW, Aarestrup FM, Lund O. 2012. Multilocus Sequence
654 Typing of Total-genome-sequenced Bacteria. J Clin Microbiol 50:1355–1361.
655 81. Wirth T, Falush D, Lan R, Colles F, Mensa P, Wieler LH, Karch H, Reeves PR, Maiden
656 MCJ, Ochman H, Achtman M. 2006. Sex and Virulence in *Escherichia coli*: An
657 Evolutionary Perspective. Mol Microbiol 60:1136–1151.
658 82. Chen I-MA, Chu K, Palaniappan K, Pillay M, Ratner A, Huang J, Huntemann M,
659 Varghese N, White JR, Seshadri R, Smirnova T, Kirton E, Jungbluth SP, Woyke T, Eloe-
660 Fadrosh EA, Ivanova NN, Kyrpides NC. 2019. IMG/M v.5.0: An Integrated Data
661 Management and Comparative Analysis System for Microbial Genomes and
662 Microbiomes. Nucleic Acids Res 47:D666–D677.
663 83. Riley LW, Remis RS, Helgerson SD, McGee HB, Wells JG, Davis BR, Hebert RJ, Olcott
664 ES, Johnson LM, Hargrett NT, Blake PA, Cohen ML. 1983. Hemorrhagic Colitis
665 Associated with a Rare *Escherichia coli* Serotype. N Engl J Med 308:681–685.
666 84. Appleyard RK. 1954. Segregation of New Lysogenic Types During Growth of a Doubly

667 Lysogenic Strain Derived from Escherichia coli K12. Genetics 39:440–452.
668 85. Blattner FR, Plunkett G, Bloch CA, Perna NT, Burland V, Riley M, Collado-Vides J,
669 Glasner JD, Rode CK, Mayhew GF, Gregor J, Davis NW, Kirkpatrick HA, Goeden MA,
670 Rose DJ, Mau B, Shao Y. 1997. The complete genome sequence of *Escherichia coli* K-12.
671 Science (80) 277:1453–1462.
672 86. Achtman M, Mercer A, Kusecek B, Pohl A, Heuzenroeder M, Aaronson W, Sutton A,
673 Silver RP. 1983. Six widespread bacterial clones among *Escherichia coli* K1 isolates.
674 Infect Immun 39:315–35.
675 87. Yorgey P, Lee J, Kördel J, Vivas E, Warner P, Jebaratnam D, Kolter R. 1994.
676 Posttranslational modifications in microcin B17 define an additional class of DNA gyrase
677 inhibitor. Proc Natl Acad Sci U S A 91:4519–4523.
678 88. Guzman L-M, Belin D, Carson MJ, Beckwith J. 1995. Tight Regulation, Modulation, and
679 High-Level Expression by Vectors Containing the Arabinose pBAD Promoter. J Bacteriol.
680 177(14):4121-4130.
681 89. Larsen RA, Thomas MG, Postle K. 1999. Protonmotive force, ExbB and ligand-bound
682 FepA drive conformational changes in TonB. Mol Microbiol 31:1809–1824.
683 90. Bolivar F, Rodriguez RL, Greene PJ, Betlach MC, Heyneker HL, Boyer HW, Crosa JH,
684 Falkow S. 1977. Construction and characterization of new cloning vehicle. II. A
685 multipurpose cloning system. Gene 2:95–113.
686
687
688
689

Figure Legends

Table 1: Bacterial isolates, plasmids and primers used in this study

***E. coli* strains**	**Characteristic(s)**	**Reference**
PA2	*stx2a*; O157:H7; Pennsylvania	(65)
PA8	*stx2a*; O157:H7; Pennsylvania	(65)
EDL933	*stx2a, stx1a*; O157:H7	(83)
C600	K12 derivative	(84)
MG1655	K12 derivative	(85)
1.0484	A phylogroup; O147; Minnesota	ECRC
0.1229	B2 phylogroup; O18:H1; Amp^R Tet^R; ST73; California	ECRC
1.0342	D phylogroup; O11; Minnesota	ECRC
1.1967	B2 phylogroup; O21; Minnesota	ECRC
1.0374	D phylogroup; O77; Minnesota	ECRC
Nissle 1917	Mutaflor; O6:H1; ST73	(28)
CFT073	UPEC; O6:H1; ST73	(27)
RS218	NMEC; O18:H7; ST95	(86)
99.0750	O36:H39; Brazil	ECRC
91.0593	O?:H10; Mexico	ECRC
90.2723	O?:H12; New York	ECRC
ZK1526	microcin B17 producing strain; W3110 Δ*lacU169 tna-2* pPY113; Amp^R	(87)

Derivatives	**Characteristic(s)**	**Antibiotic resistance**	**Reference**
0.1229Δ*mcbA*	0.1229Δ*mcbA::cat*	Cat^R Amp^R Tet^R	This study
0.122Δ*mcbABCDEFG*	0.1229Δ*mcbABCDEFG::cat*	Cat^R Amp^R Tet^R	This study
0.1229Δ6	0.1229Δp0.1229_3$^{2850\text{-}5473}$*::cat*	Cat^R Amp^R Tet^R	This study
0.1229Δ7	0.1229Δp0.1229_3$^{5426\text{-}7950}$*::cat*	Cat^R Amp^R Tet^R	This study
0.1229Δ8	0.1229Δp0.1229_3$^{8001\text{-}9950}$*::cat*	Cat^R Amp^R Tet^R	This study
0.1229Δ*hp1*	0.1229Δp0.1229_3$^{3084\text{-}3792}$*::cat*	Cat^R Amp^R Tet^R	This study
0.1229Δ*ABC*	0.1229Δp0.1229_3$^{3831\text{-}5423}$*::cat*	Cat^R Amp^R Tet^R	This study
0.1229Δ*cupin*	0.1229Δp0.1229_3$^{5426\text{-}6319}$*::cat*	Cat^R Amp^R Tet^R	This study
0.1229Δ*DUF4440*	0.1229Δp0.1229_3$^{6706\text{-}6344}$*::cat*	Cat^R Amp^R Tet^R	This study
0.1229Δ*DUF2164*	0.1229Δp0.1229_3$^{6942\text{-}6703}$*::cat*	Cat^R Amp^R Tet^R	This study
0.1229Δ*hp2*	0.1229Δp0.1229_3$^{7227\text{-}7048}$*::cat*	Cat^R Amp^R Tet^R	This study
0.1229Δ*hp3*	0.1229Δp0.1229_3$^{9099\text{-}7546}$*::cat*	Cat^R Amp^R Tet^R	This study
0.1229Δ*tolC*	0.1229Δ*tolC::cat*	Cat^R Amp^R Tet^R	This study
0.1229Δ*tolC* pBAD18::*tolC*	0.1229Δ*tolC::cat* + pBAD18::*tolC*	Cat^R Amp^R Tet^R Kan^R	This study
0.1229Δ*tolC* pBAD18	0.1229Δ*tolC::cat* + pBAD18	Cat^R Amp^R Tet^R Kan^R	This study
W3110Δ*tolC* P*recA-GFP*	W3110Δ*tolC::tet* + P*recA-GFP*	Tet^R Kan^R	(66)
MG1655 P*recA-GFP*	MG1655 P*recA-GFP*	Kan^R	This study

MG1655Δ*tonB* P*recA-GFP*	MG1655Δ*tonB::cat* + P*recA-GFP*	Cat^R Kan^R	This study
MG1655Δ*tonB* P*recA-GFP* pKP315	MG1655Δ*tonB::cat* + P*recA-GFP* + pKP215	Cat^R Kan^R Amp^R	This study
MG1655Δ*tonB* P*recA-GFP* pBAD24	MG1655Δ*tonB::cat* + P*recA-GFP* + pBAD24	Cat^R Kan^R Amp^R	This study
C600 pBR322:: p0.1229_3$^{2745\text{-}7950}$	C600 + pBR322::p0.1229_3$^{2745\text{-}7950}$	Tet^R	This study
C600 pBR322	C600 + pBR322	Amp^R Tet^R	This study
C600 p0.1229_3	C600 + p0.1229_3	Amp^R	This study

Plasmids	**Characteristic(s)**	**Antibiotic resistance**	**Reference**
p0.1229_1	114kb plasmid of 0.1229	None	This study
p0.1229_2	96kb plasmid of 0.1229	Tet^R	This study
p0.1229_3	13kb plasmid of 0.1229	Amp^R	This study
pKD3	pKD3	Cat^R, Amp^R	(68)
pKD46-Kan^R	pKD46; pCRISPR, P_{araC}-λ-red recombinase	Kan^R	Nikki Shariat
P*recA-GFP*	pMSs201 + P*recA-GFP*	Kan^R	(66)
pBAD24	pBAD24; *araC*	Amp^R	(88)
pKP315	pBAD24::*tonB*; P_{araC}	Amp^R	(89)
pBAD18	pBAD18; P_{araC}	Kan^R	(88)
pBAD18::*tolC*	pBAD18::*tolC*; P_{araC}	Kan^R	This study
pBR322	pBR322	Amp^R, Tet^R	(90)
pBR322::hp1end7	pBR322::p0.1229_3$^{2850\text{-}7950}$	Tet^R	This study

Primers

Experiment	**Primer Name**	**Sequence**	**T_a, variable time**
Δ*mcbA* & Δ*mcbABCDEFG*	mcbA-KF	atactattcagatgtcataagcattaatttcccttaaaaaaggagtccttGTGTAGGCTGGAGCTGCTTC	62°C, 100s
	mcbA-KR	ttttttaatatcagggagcaccatgctccctgaacggttaattcaacgtaCATATGAATATCCTCCTTAG	
Δ*mcbA*	mcbA-VF	GGGGCTTAAAGGGGTAGTGT	49°C, 45s
	mcbA-VR	AAGCGATTCGTCCAGTAGTTT	
Δ*mcbABCDEFG*	mcbG-KR	gtccggttctgaggaggggcccgtccgggcaaccggcgggtctactcaccCATATGAATATCCTCCTTAG	70.9°C, 2min
	mcbG-VR	CCTAACAACGCCACGACTTT	49°C, 2min
Δ*6*	6-KF	acacatttcgtacagcctttacactcggtgaattagcggccctagatgcaGTGTAGGCTGGAGCTGCTTC	67°C, 3min
	6-KR	ttaaacctcatgttttgtgatatctataatctgtgctttaggtatattatCATATGAATATCCTCCTTAG	
	6-VF	GAAGATATCGCACGCCTCTC	54.5°C, 3min
	6-VR	CGCCTGTTTGGCTATATGTG	
Δ*7*	7-KF	aatatacctaaagcacagattatagatatcacaaaacatgaggtttaaaaGTGTAGGCTGGAGCTGCTTC	70°C, 90s

	7-KR	tggagtttgtgcaggacgggagaaggaaatttctggttatcccgcaggggCATATGAATATCCTCCTTAG	
	7-VF	TTCGATGAACCGACAAAAGG	54°C, 2.5min
	7-VR	GGGTGAAAGAGGCGATGAT	
Δ8	8-KF	tttaccgcagctgcctcgcacgcttcggggatgacggtgaaaacctctgaGTGTAGGCTGGAGCTGCTTC	68°C, 90s
	8-KR	agcagacaccgctcgccgcagccgaacgaccgagtgtagctagtcagtgaCATATGAATATCCTCCTTAG	
	8-VF	CACGGAGGCATCAGTGACTA	54.9°C, 2.5min
	8-VR	CAGCCTTTTCCTGGTTCTTG	
ΔABC	ABC-KF	aattctagataacataaagcccgtaatatacgggctttaaggattataaaGTGTAGGCTGGAGCTGCTTC	64.5°C, 90s
	ABC-KR	atatttcttaaatttttctatgatttccttttttataagattattcatttCATATGAATATCCTCCTTAG	
	ABC-VF	GCGAAAAGATGTTTGGAATGA	52.7°C, 90s
	ABC-VR	TCGGGAAAGTTGTCATTTGC	
Δhp1	hp1-KF	ataaatgataactattctcatctacattcaaatatataattgggggtgttGTGTAGGCTGGAGCTGCTTC	65.7°C, 90s
	hp1-KR	aataaaattcaatttataatccttaaagcccgtatattacgggctttatgCATATGAATATCCTCCTTAG	
	hp1-VF	ACTGGCTGCAAAAACCTTGT	53.2°C, 75s
	hp1-VR	TTTCTCCTATTGAATCTTTATTGTCA	
Δcupin	cupin KF	aatatacctaaagcacagattatagatatcacaaaacatgaggtttaaaaGTGTAGGCTGGAGCTGCTTC	66.5°C, 3min
	cupin KR	agtttatatcgtatgaaaaaatctaaggggaagccccttagattaatggCATATGAATATCCTCCTTAG	
	cupin VF	AAAGAGGAAAACAAGGAAAAGCA	54°C, 2min
	cupin VR	GCATTGCTTGTGTTTCAGGG	
ΔDUF4440	DUF4440 KF	aaaaaataaaacttgaacatatataaccattaatctaaggggggcttccccGTGTAGGCTGGAGCTGCTTC	68°C, 3min
	DUF4440 KR	aggaatgttggggatagattagaggaggaattagatatgaggaaggtagtCATATGAATATCCTCCTTAG	
ΔDUF2164	DUF2164 KF	tgcattataccattcttttcttattagatttaagtctgatttaaaattagGTGTAGGCTGGAGCTGCTTC	68°C, 3min
	DUF2164 KR	tgataggaaaaatgttatattattaatttatttgtgaggcttcataaagaCATATGAATATCCTCCTTAG	
ΔDUF4440 & ΔDUF2164	DUF4440/ 2164 VF	GGCACAATGTTACGACTCAGA	55°C, 90s
	DUF4440/ 2164 VR	GTTTCAGCGGTGCGTACAAT	
Δhp2	hp2 KF	aaattacaactcaaccatactgcaacctggaatttcccaagcaagcatatGTGTAGGCTGGAGCTGCTTC	68°C, 3min
	hp2 KR	tgtctctggctggcaattcctgcgtgattcacatggctgcatagctatgcCATATGAATATCCTCCTTAG	
	hp2 VF	TCCTCTGATTCAAACTGTCCAAG	55°C, 90s
	hp2 VR	TGTTGCTGTGTTTTGCCTCT	
Δhp3	hp3 KF	aggcaaaacacagcaacaaaagacacaccagaatcgcgcccgtatgcgttGTGTAGGCTGGAGCTGCTTC	68°C, 3min

	hp3 KR	acagcgagaacaggagataagggatgaacggctgatacaggaacgcgaacCATATGAATATCCTCCTTAG	
	hp3 VF	GAATTGCCAGCCAGAGACAG	55°C, 90s
	hp3 VR	GGTCATGCAGTTGAGTCAGC	
Δ*tonB*	tonB-KF	tgcatttaaaatcgagacctggtttttctactgaaatgattatgacttcaGTGTAGGCTGGAGCTGCTTC	68.6°C, 90s
	tonB-KR	ctgttgagtaatagtcaaaagcctccggtcggaggcttttgactttctgcCATATGAATATCCTCCTTAG	
	tonB-VF	AACATACAACACGGGCACAA	54.9°C, 75s
	tonB-VR	GACGACATCGGTCAGCATTA	
Δ*tolC*	tolC-KF	aattttacagtttgatcgcgctaaatactgcttcaccacaaggaatgcaaGTGTAGGCTGGAGCTGCTTC	64.5°C, 90s
	tolC-KR	atctttacgttgccttacgttcagacggggccgaagccccgtcgtcgtcaCATATGAATATCCTCCTTAG	
	tolC-VF	CCAAATGTAACGGGCAGGTT	56°C, 2.5min
	tolC-VR	GCGTGGCGTATGGATTTTGT	
pBAD18::*tolC*	pBAD18 tolC L insert	GCTAGCGAATTCGAGCTCGGTACCCGGGGGAATCCGCAATAATTTTACAGTTTGATCGCG	62°C, 2.5min
	pBAD18 tolC R insert	GCTTGCATGCCTGCAGGTCGACTCTAGAGGATAACCCGTATCTTTACGTTGCCTTACG	
	pBAD18 tolC R plasmid	CGTAAGGCAACGTAAAGATACGGGTTATCCTCTAGAGTCGACCTGCAGGCATGCAAGC	62°C, 5min
	pBAD18 tolC L plasmid	CGCGATCAAACTGTAAAATTATTGCGGATTCCCCCGGGTACCGAGCTCGAATTCGCTAGC	
	pBAD18 F	CTGTTTCTCCATACCCGTT	45°C, 2.25min
	pBAD18 R	CTCATCCGCCAAAACAG	
pBR322:: p0.1229_3$^{2745-7950}$	pBR322 hp1 upstream L insert	GTATATATGAGTAAACTTGGTCTGACAGCATTAAAAGAGGCGTCAGAGGCAGAAAACG	56°C, 4min
	pBR322 end 7 R insert	GCGGCATTTTGCCTTCCTGTTTTTGCGAAATCGGCAACGGTGATTCCCTATCAGGG	
	pBR322 end 7 R plasmid	CCCTGATAGGGAATCACCGTTGCCGATTTCGCAAAAACAGGAAGGCAAAATGCCGC	62°C, 4min
	pBR322 hp1 upstream L plasmid	CGTTTTCTGCCTCTGACGCCTCTTTTAATGCTGTCAGACCAAGTTTACTCATATATAC	
	pBR322-F	TTTGCAAGCAGCAGATTACG	54.4°C, 2min
	pBR322-R	GCCTCGTGATACGCCTATTT	

692 ECRC, Penn State *E. coli* Reference Center; Amp^{R}, ampicillin resistant; Cat^{R}, chloramphenicol

693 resistant; Kan^{R}, kanamycin resistant; Tet^{R}, tetracycline resistant; *stx2a*, Shiga toxin 2a; *stx1a*,

694 Shiga toxin 1a; P_{araC}, arabinose inducible promoter; T_a, amplification temperature; KF, knockout
695 forward; KR, knockout reverse; VF, verification forward; VR, verification reverse. Note: For the
696 KF or KR primers, the lower-case letters indicate homologous regions to the target gene and the
697 upper-case letters indicate the primer for the antibiotic resistant cassette. Superscript numbers
698 indicate regions knocked out.
699
700 Fig. 1: PA2 was grown with various *E. coli* strains and Stx2a levels were measured using the R-
701 ELISA. LB refers to PA2 grown in mono-culture. One-way ANOVA was used and bars marked
702 with an asterisk were significantly higher than LB (Dunnett's test, $p < 0.05$).
703
704 Fig. 2: The Stx2a levels (A) and fluorescence (B) of non-pathogenic *E. coli*, after PA2 growth in
705 cell-free supernatant or W3110Δ*tolC* P*recA-gfp* co-culture, respectively. Samples were
706 normalized to cell density, OD_{600} or OD_{620}, for Stx2a or fluorescence, respectively. One-way
707 ANOVA was used and levels marked with an asterisk were significantly higher than LB
708 (Dunnett's test, $p < 0.05$). The Stx2a levels (C) of PA2 grown in 0.1229 cell-free supernatant
709 (2C-left) or LB (2C-right) with or without heat and Proteinase K treatments. Two-way ANOVA
710 was used and bars marked with an asterisk were significantly lower than untreated 0.1229 or LB
711 (Dunnett's test, $p < 0.05$).
712
713 Fig. 3: Plasmid comparisons of individual 0.1229 plasmids and publicly available plasmids from
714 NCBI by BLAST and visualized with BRIG. The colored rings indicate sequence similarity and
715 the outer grey ring denotes annotated ORFs. The MccB17 operon is labeled *mcbA-mcbG*, and
716 five antimicrobial resistance genes, macrolide (*mph(A)*), tetracycline (*tet(A)*), sulphonamide

(*sul1*), aminoglycoside (*aadA2*), and trimethoprim (*dfrA12*) were identified (B). Ampicillin resistance gene (*blaTEM-1B*) and four ORFs, *hp1*, *abc*, *cupin* and *hp2* are also labeled (C). NCBI accession numbers are pUTI89 (CP000244), pRS218 (CP007150), pECO-fce (CP015160), pSF-173-1 (CP012632), pHUSEC41-3 (NC_018997), and pEC16II (KU932034).

Fig. 4: The Stx2a levels (A) and fluorescence (B) of 0.1229, its MccB17 knockouts and ZK1526, after PA2 growth in cell-free supernatant or W3110Δ*tolC* P*recA-gfp* co-culture, respectively. Samples were normalized to cell density, OD_{600} or OD_{620}, for Stx2a or fluorescence, respectively. One-way ANOVA was used and bars marked with an asterisk were significantly lower than 0.1229 (Dunnett's test, $p < 0.05$).

Fig. 5: PA2 was grown in the cell-free supernatant of 0.1229, C600 containing p0.1229_3 and C600. Stx2a levels were measured using the R-ELISA. LB refers to PA2 grown in LB broth. One-way ANOVA was used and bars marked with an asterisk were significantly higher than LB (Fisher's LSD test, $p < 0.05$).

Fig. 6: PA2 was grown in the cell-free supernatant of 0.1229 knockouts (A & C). Portion of p0.1229_3 is depicted with predicted open reading frames (ORFs) (B). The colored triangles indicate the name of the regional knockout., PA2 grown in the supernatant of a C600 strain containing a portion of p0.1229_3 (pBR322::p0.1229_3$^{2745\text{-}7950}$) (C). Stx2a levels measured using the R-ELISA. LB refers to PA2 grown in LB broth. One-way ANOVA was used and bars marked with an asterisk were significantly lower than 0.1229 (Fisher's LSD test, $p < 0.05$).

Fig. 7: W3110Δ*tolC* P*recA-gfp* was grown in co-culture with 0.1229, 0.1229Δ*tolC* and 0.1229Δ*tolC* pBAD18 containing strains, and fluorescence was measured. Samples were normalized to cell density, OD_{620}. One-way ANOVA was used and bars marked with an asterisk were significantly higher than LB (Dunnett's test, $p < 0.05$).

Fig. 8: Plasmid expressing P*recA-gfp* was electroporated into MG1655, MG1655Δ*tonB,* MG1655Δ*tonB* pBAD24 and MG1655Δ*tonB* pBAD24::*tonB*. These strains were grown in co-culture with 0.1229, or by themselves (LB). Two-way ANOVA was used and bars marked with an asterisk were significantly higher than their respective monoculture control (Dunnett's test, $p < 0.05$).

Fig. 9: PA2 was grown in the cell-free supernatant of 0.1229 and three human fecal *E. coli* isolates (A). Stx2a levels measured using the R-ELISA. LB refers to PA2 grown in LB broth. One-way ANOVA was used and bars marked with an asterisk were significantly higher than LB (Dunnett's test, $p < 0.05$). p0.1229_3 was compared to the contigs of 99.0750, 91.0593 and 90.2723 using BLAST and visualized using BRIG (B).

Fig. S1: W3110Δ*tolC* P*recA-gfp* was grown with 0.1229 and 0.1229 regional (A) or individual ORF (B) knockouts, or alone indicated by LB. One-way ANOVA was used and levels marked with an asterisk were significantly lower than 0.1229 (Dunnett's test, $p < 0.05$).

Fig. S2: A portion of p0.1229_3 is compared to *K. pneumoniae* TR152 (SAMEA3729690), *S. sonnei* 143778 (SAMEA2057991), *E. coli* HUSEC41 (PRJEA73977), *E. coli* HVH206

(SAMN01885845). * indicates one amino acid (aa) difference in that ORF. # indicates seven aa differences in that ORF. The grey shaded region is >99.6% nucleotide identical between all strains.

Fig. S3: Hp1 protein was compared to genomes on Integrated Microbial Genomes & Microbiomes of DOE's Joint Genome Institute. Using BLASTp, isolates were compared, sorted by BIT score, and then one strain from the top ten species were selected. % identity ranged from 32 to 68%. Hp1 homologs are colored in red. 8/10 have ABC transporters adjacent to Hp1, colored in light blue or maroon. 9/10 have an annotated region similar to Cupin, colored in pale yellow, typically adjacent to the ABC transporter. DUF2164 is found in five strains, one in the reverse direction than Hp1. The *Burkholderia cepacia* strain encodes L-arabinose system upstream of Hp1. The bracket indicates groupings of Hp1, ABC and Cupin.

Fig. S4: W3110Δ*tolC* P*recA-gfp* was grown with 0.1229 or 101 human fecal isolates from the *E. coli* Reference Center at Penn State. As a control, W3110 P*recA-GFP* was grown by itself indicated by LB. One-way ANOVA was used and levels marked with an asterisk were significantly higher than LB (Dunnett's test, $p < 0.05$).

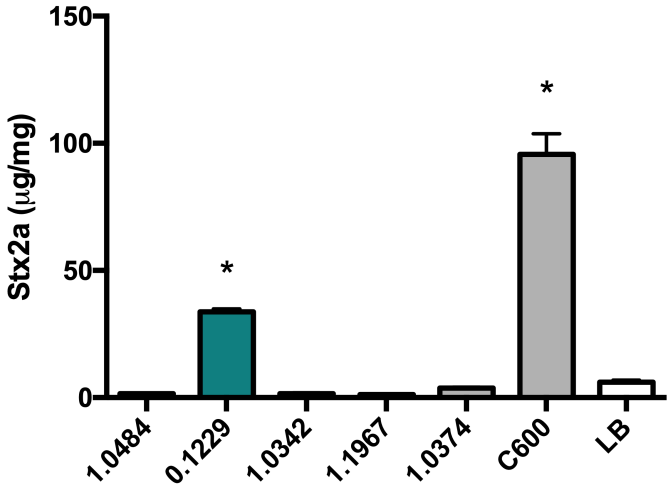

Fig. 1: PA2 was grown with various *E. coli* strains and Stx2a levels were measured using the R-ELISA. LB refers to PA2 grown in mono-culture. One-way ANOVA was used and bars marked with an asterisk were significantly higher than LB (Dunnett's test, $p < 0.05$).

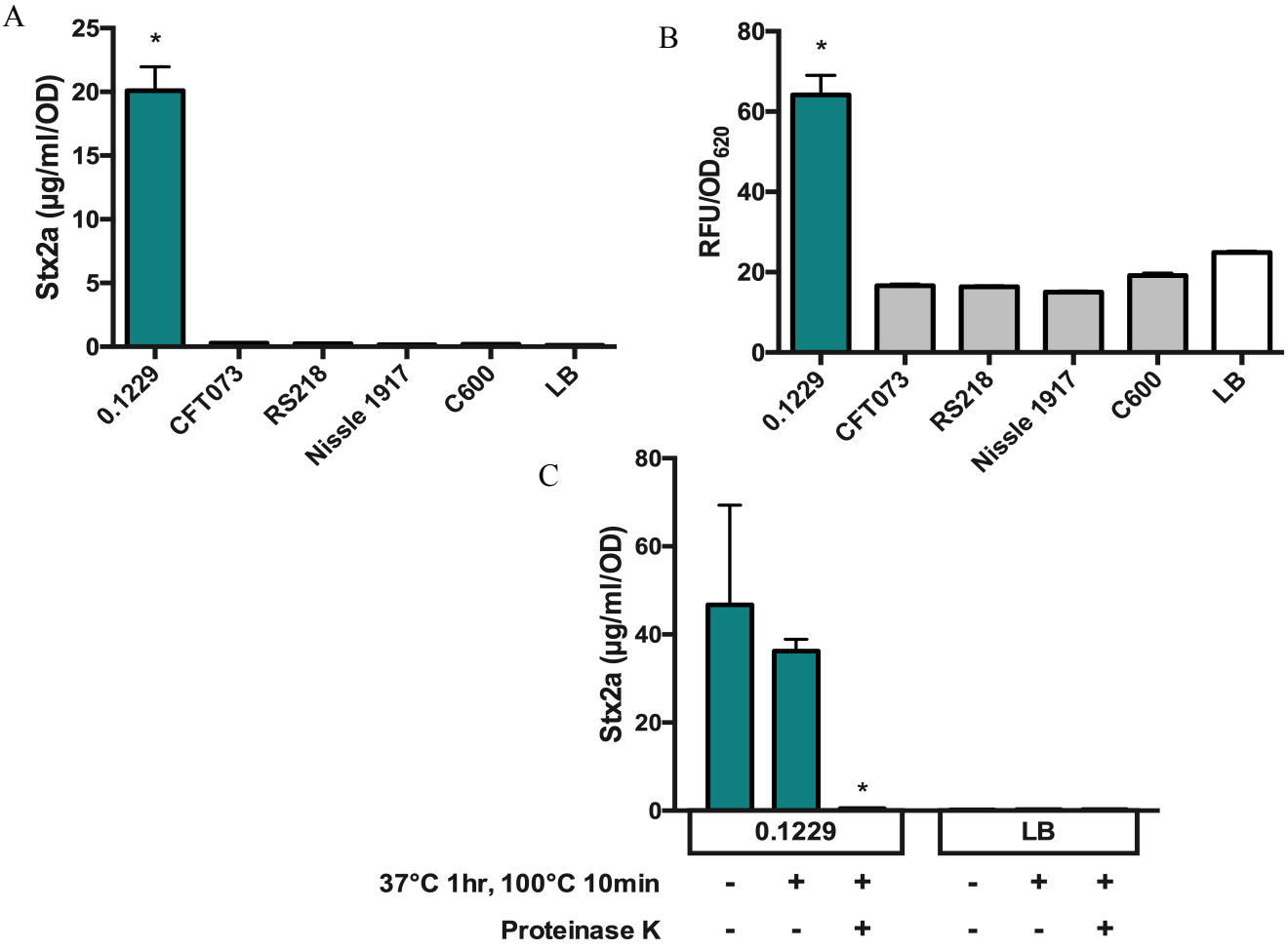

Fig. 2: The Stx2a levels (A) and fluorescence (B) of non-pathogenic *E. coli*, after PA2 growth in cell-free supernatant or W3110Δ*tolC* P*recA-gfp* co-culture, respectively. Samples were normalized to cell density, OD_{600} or OD_{620}, for Stx2a or fluorescence, respectively. One-way ANOVA was used and levels marked with an asterisk were significantly higher than LB (Dunnett's test, $p < 0.05$). The Stx2a levels (C) of PA2 grown in 0.1229 cell-free supernatant (2C-left) or LB (2C-right) with or without heat and Proteinase K treatments. Two-way ANOVA was used and bars marked with an asterisk were significantly lower than untreated 0.1229 or LB (Dunnett's test, $p < 0.05$).

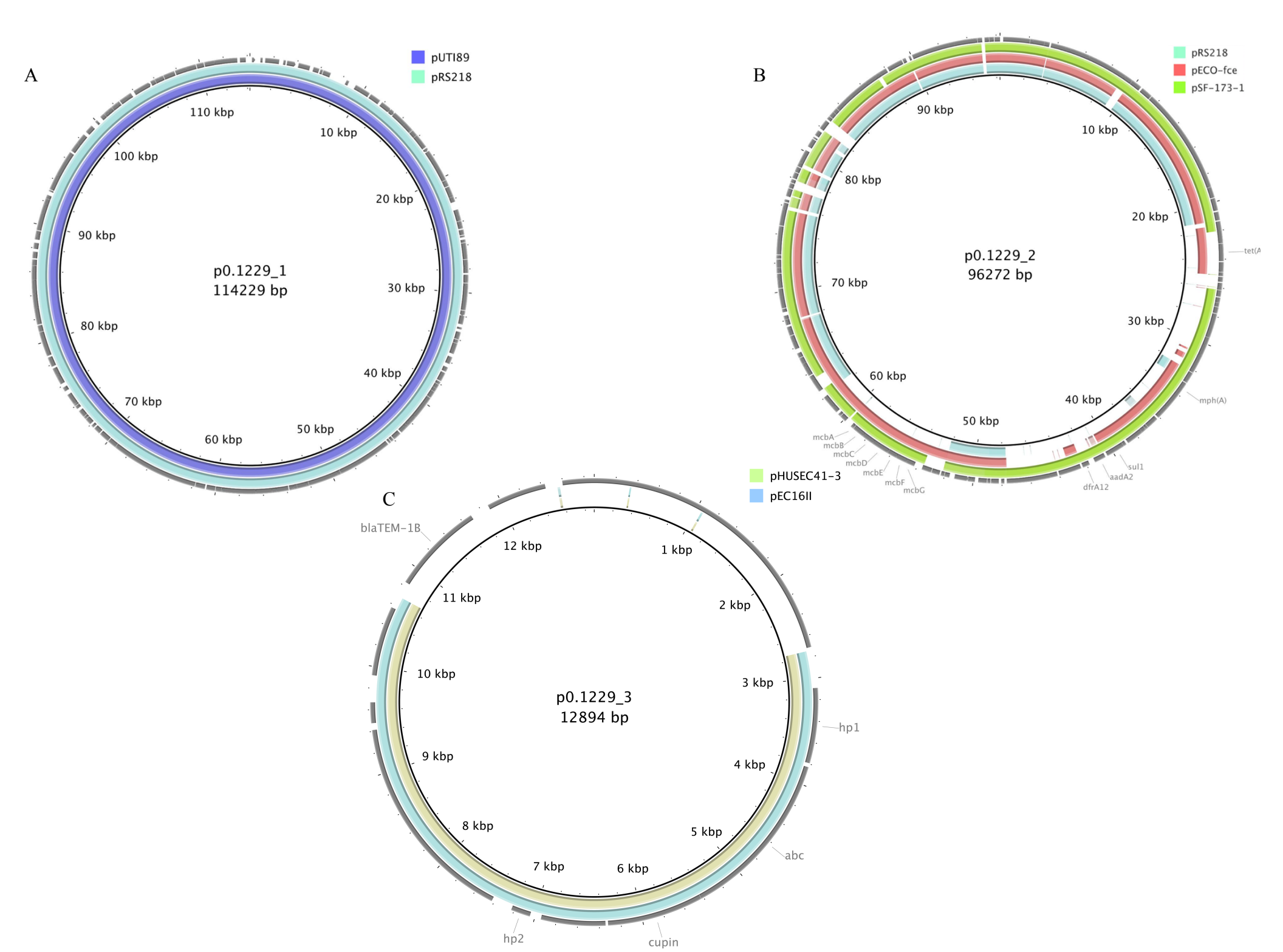
A
pUTI89
pRS218
p0.1229_1
114229 bp
10 kbp
20 kbp
30 kbp
40 kbp
50 kbp
60 kbp
70 kbp
80 kbp
90 kbp
100 kbp
110 kbp
B
pRS218
pECO-fce
pSF-173-1
p0.1229_2
96272 bp
10 kbp
20 kbp
30 kbp
40 kbp
50 kbp
60 kbp
70 kbp
80 kbp
90 kbp
tet(A
mph(A)
sul1
aadA2
dfrA12
mcbA
mcbB
mcbC
mcbD
mcbE
mcbF
mcbG
pHUSEC41-3
pEC16II
C
p0.1229_3
12894 bp
1 kbp
2 kbp
3 kbp
4 kbp
5 kbp
6 kbp
7 kbp
8 kbp
9 kbp
10 kbp
11 kbp
12 kbp
blaTEM-1B
hp1
abc
cupin
hp2

Fig. 3: Plasmid comparisons of individual 0.1229 plasmids and publicly available plasmids from NCBI by BLAST and visualized with BRIG. The colored rings indicate sequence similarity and the outer grey ring denotes annotated ORFs. The MccB17 operon is labeled *mcbA-mcbG*, and five antimicrobial resistance genes, macrolide (*mph(A)*), tetracycline (*tet(A)*), sulphonamide (*sul1*), aminoglycoside (*aadA2*), and trimethoprim (*dfrA12*) were identified (B). Ampicillin resistance gene (*blaTEM-1B*) and four ORFs, *hp1*, *abc*, *cupin* and *hp2* are also labeled (C). NCBI accession numbers are pUTI89 (CP000244), pRS218 (CP007150), pECO-fce (CP015160), pSF-173-1 (CP012632), pHUSEC41-3 (NC_018997), and pEC16II (KU932034).

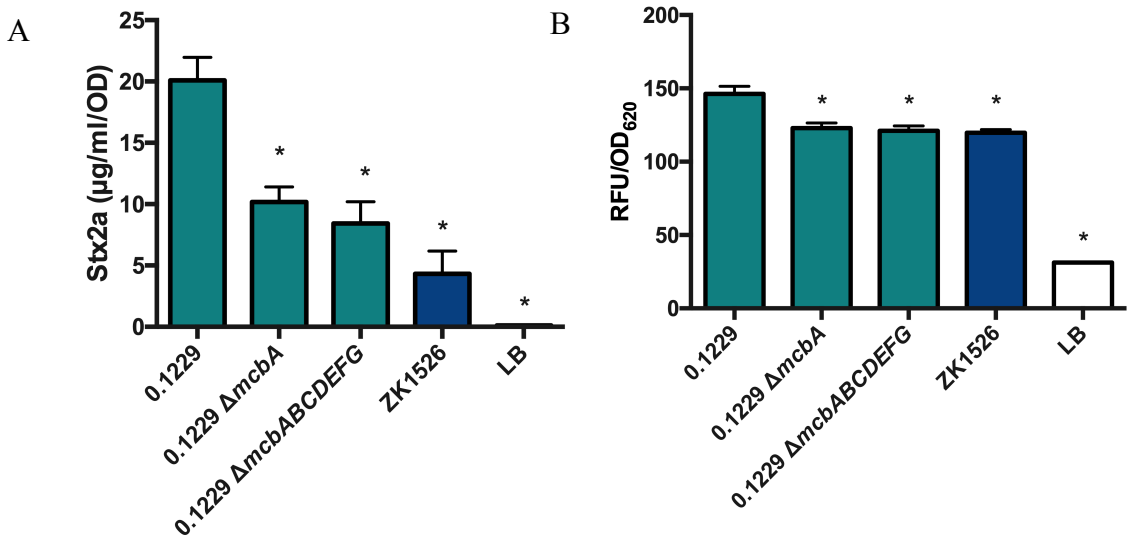

Fig. 4: The Stx2a levels (A) and fluorescence (B) of 0.1229, its MccB17 knockouts and ZK1526, after PA2 growth in cell-free supernatant or W3110Δ*tolC* P*recA-gfp* co-culture, respectively. Samples were normalized to cell density, OD_{600} or OD_{620}, for Stx2a or fluorescence, respectively. One-way ANOVA was used and bars marked with an asterisk were significantly lower than 0.1229 (Dunnett's test, $p < 0.05$).

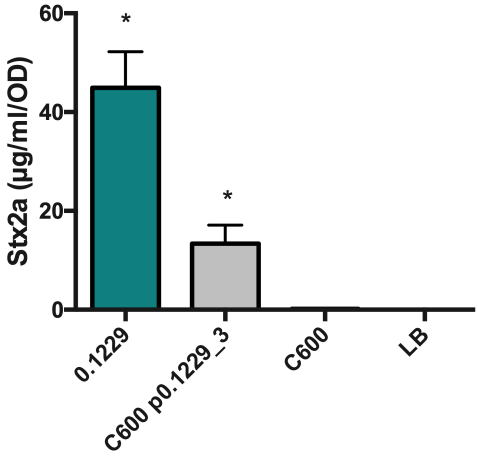

Fig. 5: PA2 was grown in the cell-free supernatant of 0.1229, C600 containing p0.1229_3 and C600. Stx2a levels were measured using the R-ELISA. LB refers to PA2 grown in LB broth. One-way ANOVA was used and bars marked with an asterisk were significantly higher than LB (Fisher's LSD test, $p < 0.05$).

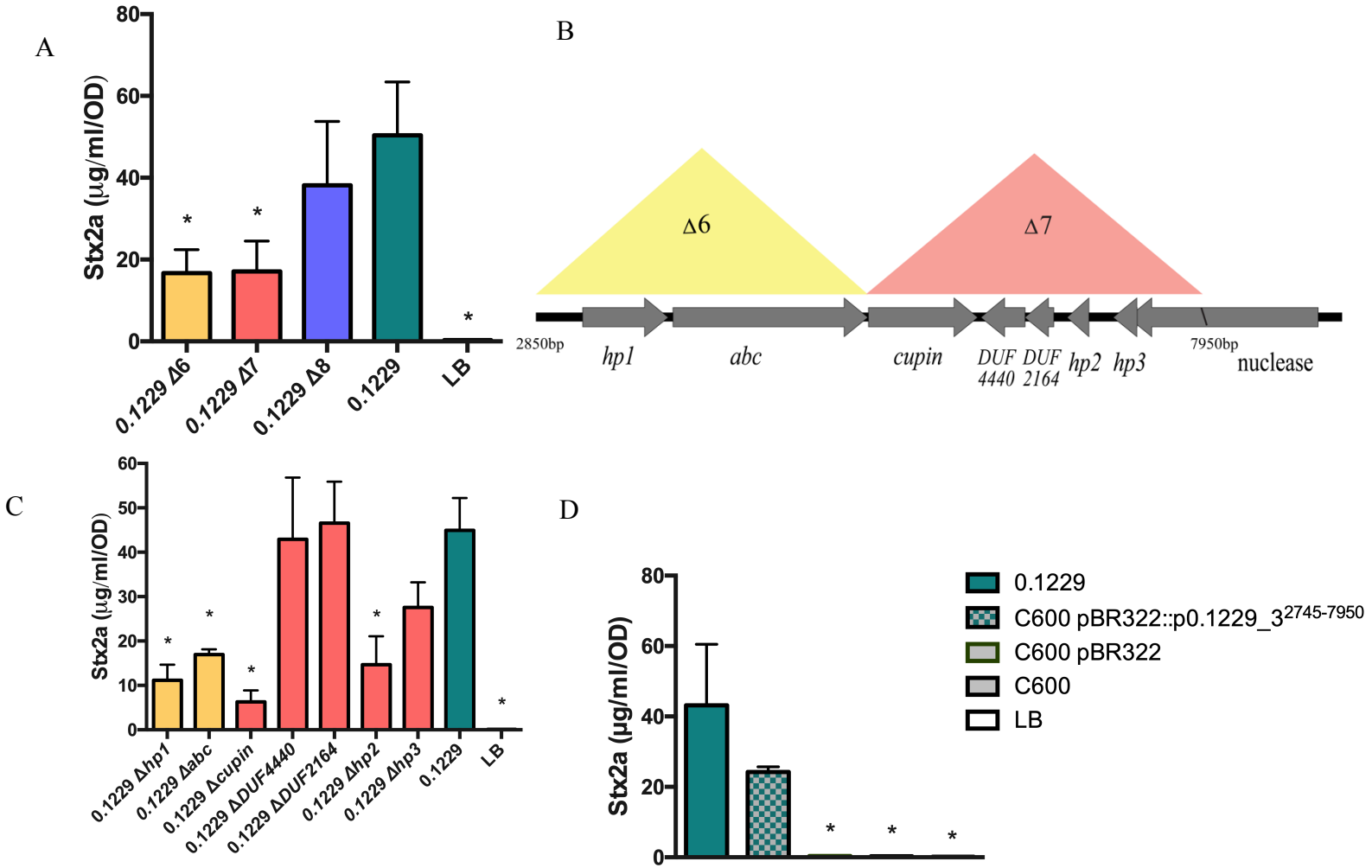

Fig. 6: PA2 was grown in the cell-free supernatant of 0.1229 knockouts (A & C). Portion of p0.1229_3 is depicted with predicted open reading frames (ORFs) (B). The colored triangles indicate the name of the regional knockout., PA2 grown in the supernatant of a C600 strain containing a portion of p0.1229_3 (pBR322::p0.1229_3$^{2745\text{-}7950}$) (C). Stx2a levels measured using the R-ELISA. LB refers to PA2 grown in LB broth. One-way ANOVA was used and bars marked with an asterisk were significantly lower than 0.1229 (Fisher's LSD test, $p < 0.05$).

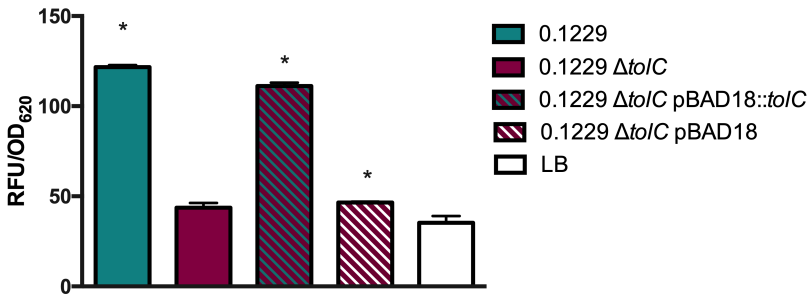

Fig. 7: W3110Δ*tolC* P*recA-gfp* was grown in co-culture with 0.1229, 0.1229Δ*tolC* and 0.1229Δ*tolC* pBAD18 containing strains, and fluorescence was measured. Samples were normalized to cell density, OD_{620}. One-way ANOVA was used and bars marked with an asterisk were significantly higher than LB (Dunnett's test, $p < 0.05$).

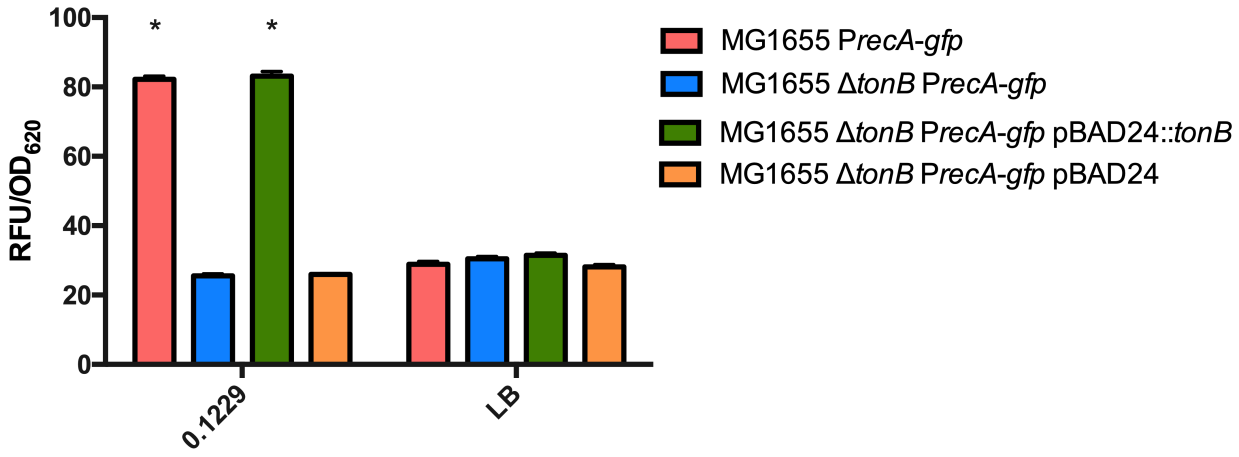

Fig. 8: Plasmid expressing P*recA-gfp* was electroporated into MG1655, MG1655Δ*tonB,* MG1655Δ*tonB* pBAD24 and MG1655Δ*tonB* pBAD24::*tonB*. These strains were grown in co-culture with 0.1229, or by themselves (LB). Two-way ANOVA was used and bars marked with an asterisk were significantly higher than their respective monoculture control (Dunnett's test, $p < 0.05$).

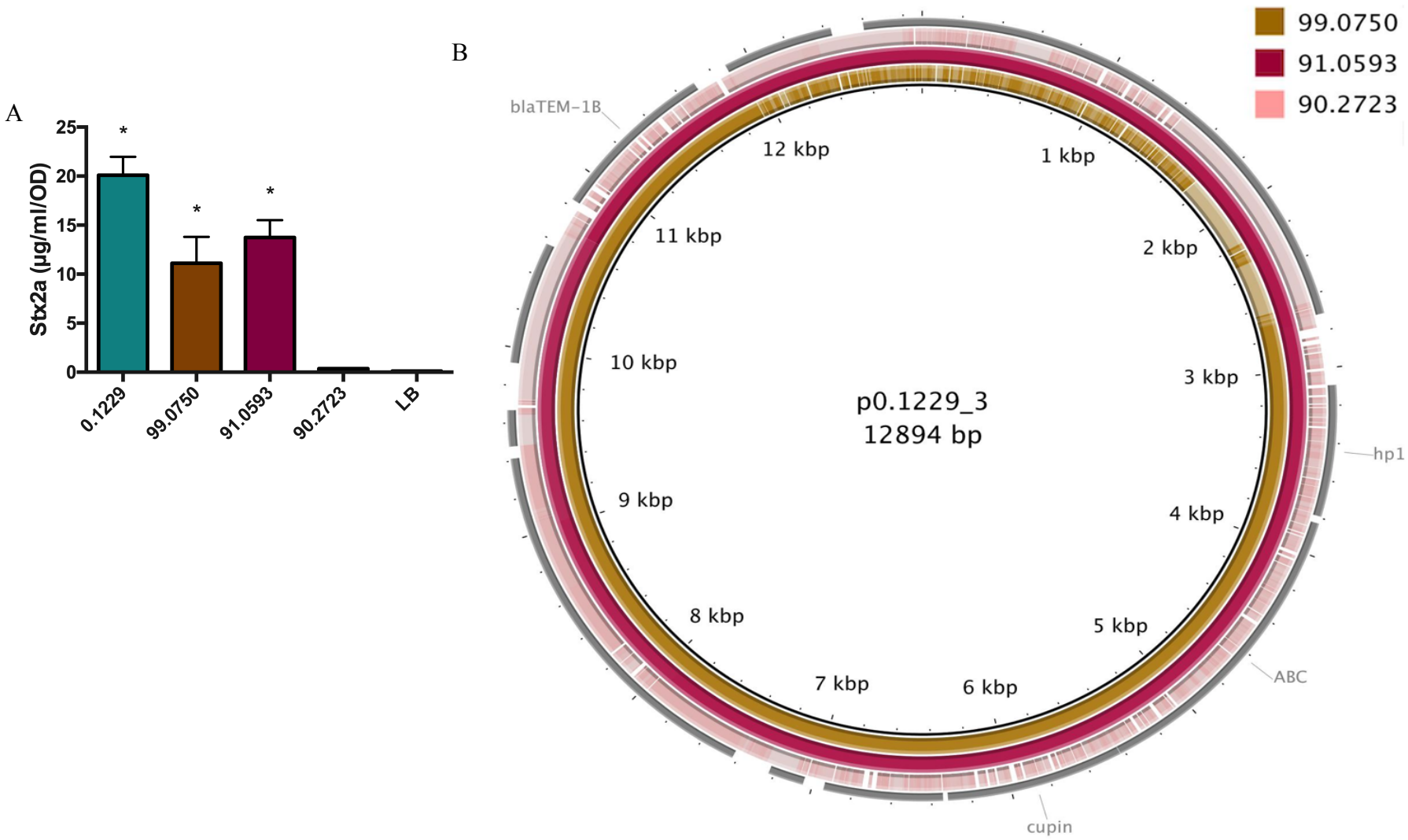

Fig. 9: PA2 was grown in the cell-free supernatant of 0.1229 and three human fecal *E. coli* isolates (A). Stx2a levels measured using the R-ELISA. LB refers to PA2 grown in LB broth. One-way ANOVA was used and bars marked with an asterisk were significantly higher than LB (Dunnett's test, $p < 0.05$). p0.1229_3 was compared to the contigs of 99.0750, 91.0593 and 90.2723 using BLAST and visualized using BRIG (B).